



Electricity Markets & Policy
Energy Analysis & Environmental Impacts Division
Lawrence Berkeley National Laboratory

Are coupled renewable-battery power plants more valuable than independently sited installations?

Will Gorman , Cristina Crespo Montañés, Andrew Mills, James Hyungkwan Kim, Dev Millstein, Ryan Wisler

May 2021

This is a pre-print version of a journal article currently in peer review.



DISCLAIMER

This document was prepared as an account of work sponsored by the United States Government. While this document is believed to contain correct information, neither the United States Government nor any agency thereof, nor The Regents of the University of California, nor any of their employees, makes any warranty, express or implied, or assumes any legal responsibility for the accuracy, completeness, or usefulness of any information, apparatus, product, or process disclosed, or represents that its use would not infringe privately owned rights. Reference herein to any specific commercial product, process, or service by its trade name, trademark, manufacturer, or otherwise, does not necessarily constitute or imply its endorsement, recommendation, or favoring by the United States Government or any agency thereof, or The Regents of the University of California. The views and opinions of authors expressed herein do not necessarily state or reflect those of the United States Government or any agency thereof, or The Regents of the University of California.

Ernest Orlando Lawrence Berkeley National Laboratory is an equal opportunity employer.

COPYRIGHT NOTICE

This manuscript has been authored by an author at Lawrence Berkeley National Laboratory under Contract No. DE-AC02-05CH11231 with the U.S. Department of Energy. The U.S. Government retains, and the publisher, by accepting the article for publication, acknowledges, that the U.S. Government retains a non-exclusive, paid-up, irrevocable, worldwide license to publish or reproduce the published form of this manuscript, or allow others to do so, for U.S. Government purposes.

Are coupled renewable-battery power plants more valuable than independently sited installations?

Will Gorman^{1*}, Cristina Crespo Montañés¹, Andrew Mills¹, James Hyungkwan Kim¹, Dev Millstein¹, Ryan Wisner¹

ABSTRACT. Coupled renewable-battery powerplants differ from the traditional concept of independent siting of electricity resources within transmission networks. Prior research on the value proposition and cost savings from coupling did not consider the geographic constraint of co-location. This paper fills the gap by assessing how pricing volatility differences between nodes within electricity markets impact the system value of coupled renewable-battery projects as compared to independent VRE and battery installations. We use wholesale power market prices from 2012–2019 across the seven main U.S. independent system operators (ISOs) with a linear optimization program to compare the electricity market value of coupled projects to the value of the same underlying sub-components, deployed separately. We find that additional value from adding a 4-hour battery sized to 50% of renewable-plant nameplate capacity is \$10/MWh across ISOs on average. The highest boost occurs in California (\$15/MWh), where the value of adding storage to solar rises over time in tandem with increased solar penetration in the region. If renewables and batteries are deployed independently, we estimate that \$12.5/MWh of additional value could be achieved because of more flexibility on battery siting and operation. The \$12.5/MWh coupling penalty is reduced to \$1.6/MWh when considering alternative approaches to integrating battery storage. This result implies that renewable-battery power plants will play an increasing role in electricity systems if they can be built for \$2–\$13/MWh less than independent projects of comparable size. However, the wide regional variation in coupling penalties, along with the importance of conditions captured in our sensitivity cases, suggests the tradeoff between coupling penalties and savings will vary by situation. Therefore, roles exist for independent and coupled projects from a system optimization perspective.

KEYWORDS. Hybrids; solar; wind; battery; transmission congestion; siting decision

Acronyms: AC = alternating current, CAISO = California Independent System Operator, DAH = day-ahead, DC = direct current, EIA = U.S. Energy Information Administration, ERCOT = Electric Reliability Council of Texas, FERC = Federal Energy Regulatory Commission, ILR = inverter loading ratio, ISO = independent system operator, ISO-NE = ISO New England, ITC = investment tax credit, LCOE = levelized cost of electricity, LMP = locational marginal price, MISO = Midcontinent Independent System Operator, NREL = National Renewable Energy Laboratory, NYISO = New York Independent System Operator, POI = point of interconnection, PJM = PJM

¹ Lawrence Berkeley National Laboratory, 1 Cyclotron Road, MS 90-4000, Berkeley, CA 94720, USA

*Corresponding author, wgorman@lbl.gov

Interconnection, PTC = production tax credit, PV = photovoltaic(s), RE = renewable energy, RTO = regional transmission organization, SAM = System Advisor Model, SPP = Southwest Power Pool, VRE = variable renewable energy

1. Introduction

Technology improvements, cost reductions, and policy support have driven rapid growth of variable renewable energy (VRE) technologies, such as wind and solar [1]. To meet Paris Agreement climate targets, deployment of these resources must increase substantially [2]. Many researchers have studied the impact of high VRE levels on electricity grids [3,4]. These studies identify challenges with high-VRE grids including, but not limited to, increased flexibility requirements and long-term VRE value deflation [5–10].

Energy storage technologies could mitigate these concerns, and a large literature addresses the synergies between high VRE penetrations and storage development. Much of this literature focuses on deploying storage as a system asset, modeling storage capabilities at an aggregated level (e.g., by state, independent system operator [ISO], balancing authority) without considering variation due to transmission constraints [11–16]. This focus aligns with the conventional wisdom regarding operation of networked electricity grids: site facilities independently, at high system-value locations, and control them at a regional level using cost-optimized dispatch via system operators (ISOs and regional transmission organizations [RTOs]) leveraging transmission networks (Figure 1-1, left) [17]. This approach focuses on balancing geographically dispersed electricity loads and generation assets. Aligned with this thinking, many researchers and industry participants emphasize that market footprints enabling balancing over larger geographic territories would lead to more efficient VRE integration [18–20].

Less attention, however, has been given to the recent commercial interest in coupled (or “hybrid”) configurations, which involve pairing battery storage technologies directly with VRE technologies at the same geographic location (Figure 1-1, right). At the end of 2020, 34% of solar and 6% of wind projects by capacity were being developed with a co-located battery storage unit, according to the largest U.S. interconnection queues (Table 1-1).² Proposed development is highest in the West, where 70%–90% of proposed solar is paired with storage (compared to 5%–20% in the East), suggesting a regional driver of co-location. In California Independent System Operator (CAISO) territory, 64% of all proposed battery storage is paired with a generator [21].

² These interconnection queues cover roughly 85% of load in the United States.

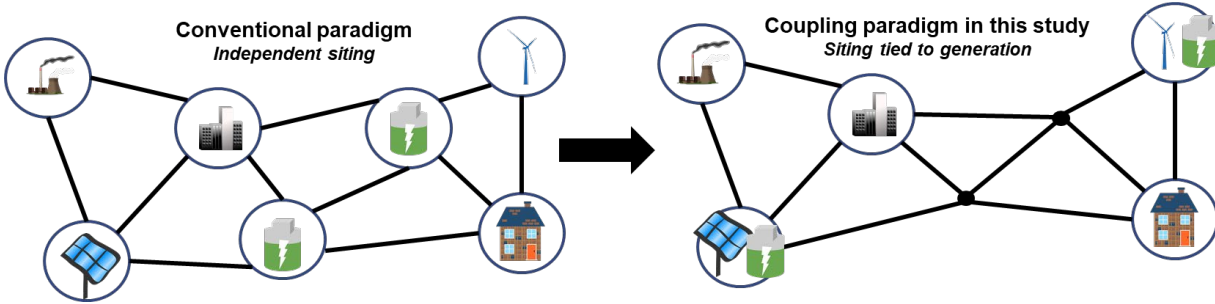


Figure 1-1: Depiction of VRE operational paradigms in electricity networks

Region	Percentage of Proposed Technology Coupling in Each Region (by capacity)		
	Solar	Wind	Battery ³
CAISO	89%	37%	64%
ERCOT	21%	6%	37%
SPP	22%	4%	38%
MISO	18%	5%	N/A
PJM	19%	1%	N/A
NYISO	5%	0%	2%
ISO-NE	12%	0%	N/A
West (non-ISO)	69%	14%	N/A
Southeast (non-ISO)	13%	0%	N/A
TOTAL	34%	6%	N/A

Table 1-1: Coupling percentage by technology in interconnection queues as of the end of 2020

This paper aims to illuminate the coupling constraints resulting from renewable-battery project development and to identify the importance of the various drivers of coupled projects. In particular, we analyze the drivers of the regional concentration of proposed coupled development, and we explore the extent to which the traditional concept of independently siting resources may not fully apply to VRE resources and storage technologies.

We focus on the system value battery storage provides within electricity markets. Storage value tends to be higher where there is more pricing volatility [22]. We explore how pricing volatility differences between nodes within electricity markets may impact coupling and battery development decisions. We estimate the opportunity cost associated with siting storage at a VRE location, rather than siting storage at a different, potentially higher-value location [23]. In a coupled configuration, storage operation may be further restricted by shared interconnection

³ N/A values signify that region does not provide enough information to calculate this statistic.

capacity or requirements to charge from the VRE rather than the grid. We aim to quantify the coupling constraints associated with such co-location and operational restrictions.

Previous research identified several drivers of increased co-location including policy incentives, construction cost synergies, mitigation of slow interconnection processes, and operational synergies through co-optimization [24,25]. However, this research did not systematically compare these benefits to all of the following aspects of coupling constraints: (1) reduced options in the geographic siting of storage, (2) increased operational constraints of sharing an inverter or grid interconnection capacity, which can reduce a coupled project's ability to schedule services during the highest-value times, and (3) restrictions on grid charging.

We use recent wholesale power market prices to calculate the energy, capacity, and ancillary service revenue of coupled projects that are physically co-located, compared with the revenue of the same underlying sub-components (VRE generator and battery storage) deployed separately. We then put these system value estimates in the context of sparse estimates of cost savings from coupling described in previous research, and we show conditions under which the project-development cost savings can outweigh constraints that limit coupling value.

Although many different configurations and technology combinations can be coupled [26], this article focuses on battery storage projects physically sited with utility-scale wind and photovoltaics (PV) owing to the recent commercial interest in this particular use case [21]. We do not study technologies that are virtual or based on distributed energy resources, nor do we evaluate potential participation models that are being developed to integrate coupled technologies into wholesale markets [27].

Instead, we focus on the physical combination of VRE and batteries and create a self-scheduled dispatch profile based on historical prices. This framing allows us to investigate how both coupling and pricing volatility via transmission constraints affect the market value of storage at different locations within wholesale electricity markets. The geographic and temporal variance of this market value drives location-specific battery project development, so it is most relevant for answering our research questions.

The remainder of the article proceeds as follows. Section 2 discusses the prior literature related to VRE system value estimation and grid planning and then identifies the specific research gaps we fill with our work. Section 3 describes the key conceptual framework comparing coupled projects to independent systems while outlining the optimization model developed. Section 4 summarizes our quantification of the system values and penalties of coupling. Section 5 contextualizes our results within current market development activities, comparing system value to system costs; this section raises important issues related to future VRE and coupled project development. Section 6 concludes and identifies open research questions.

2. Background

This paper contributes to two major strands of literature related to integrating VRE technologies onto electrical grids: (1) estimating utility-scale VRE and storage electricity market value (“system value” studies), and (2) optimal siting of and planning for utility-scale generation assets (“grid planning” studies). Within both these literatures, prior work focused either on coupled projects or independent technologies separately without applying a consistent framework to compare their value relative to each other across wide market regions. Our implementation of a consistent valuation framework combined with our wide geographic scope allows us to provide new information on the constraints involved with co-locating VRE and battery systems.

Much of the system value literature focuses on analyzing wholesale market prices while considering the inherent variability of wind speeds and solar irradiance [9,28]. In most regions, wholesale electricity market prices are split between energy, capacity, and ancillary service products, thus incentivizing resources to contribute toward meeting various electricity system needs [29]. These prices reflect competitive wholesale procurement and therefore the underlying value of instantaneously balancing supply and demand in electricity markets [17]. For standalone VRE technologies, the system value literature focuses on how weather dependence affects the system value of renewables compared to the average power prices at various VRE penetration levels [30]. Hirth finds that wind power system value drops from 110% of the average power price to 50% as wind penetration increases to 30% of total electricity consumption in Europe [8]. Mills and Wiser find that the system value of PV drops from 127% of the average power price to 36% as solar penetration reaches 30% in California [6]. Millstein finds that the 2019 energy value of wind or PV was 30% to 40% below the regional average price in regions that exceeded 20% penetration. Solar value reductions are primarily driven by the output profile, while wind value reductions are driven by both profile and within-market congestion, depending on the region [31].

Given the ability of storage to mitigate wind and solar variability and value deflation, more recent research has examined the system value of grid-scale battery storage [32–34]. Byrne et al. find significant revenue potential for storage market arbitrage assuming perfect foresight [35], and McPherson et al. show that storage can be profitable even using more realistic day-ahead scheduling algorithms [36]. This literature rarely evaluates coupled technologies, focusing instead on standalone battery system value. A few recent studies have begun to explore the value of coupled projects but do not correspondingly evaluate how these emerging configurations compare to the independent system value of standalone configurations, especially considering the broad geographic context of current market-based generator investments [37–40]. Denholm finds that PV-storage coupled projects can be more or less profitable than independent configurations depending on constraints considered, but analyzes only a single location in California [41].

The grid planning literature takes a broader market context to evaluate siting and planning decisions, considering a variety of electric system technologies [42,43]. Most of these studies use capacity-expansion methods and focus on the important role of transmission and balancing authorities to manage the variability of VRE technologies [44,45]. Generally, these studies show

that a portfolio of resources including VRE, storage, and transmission is needed to transition to a low-carbon energy system [46,47]. In contrast to system value studies, grid planning studies develop a cost-benefit framework to compare multiple generation types given a number of electric system constraints.

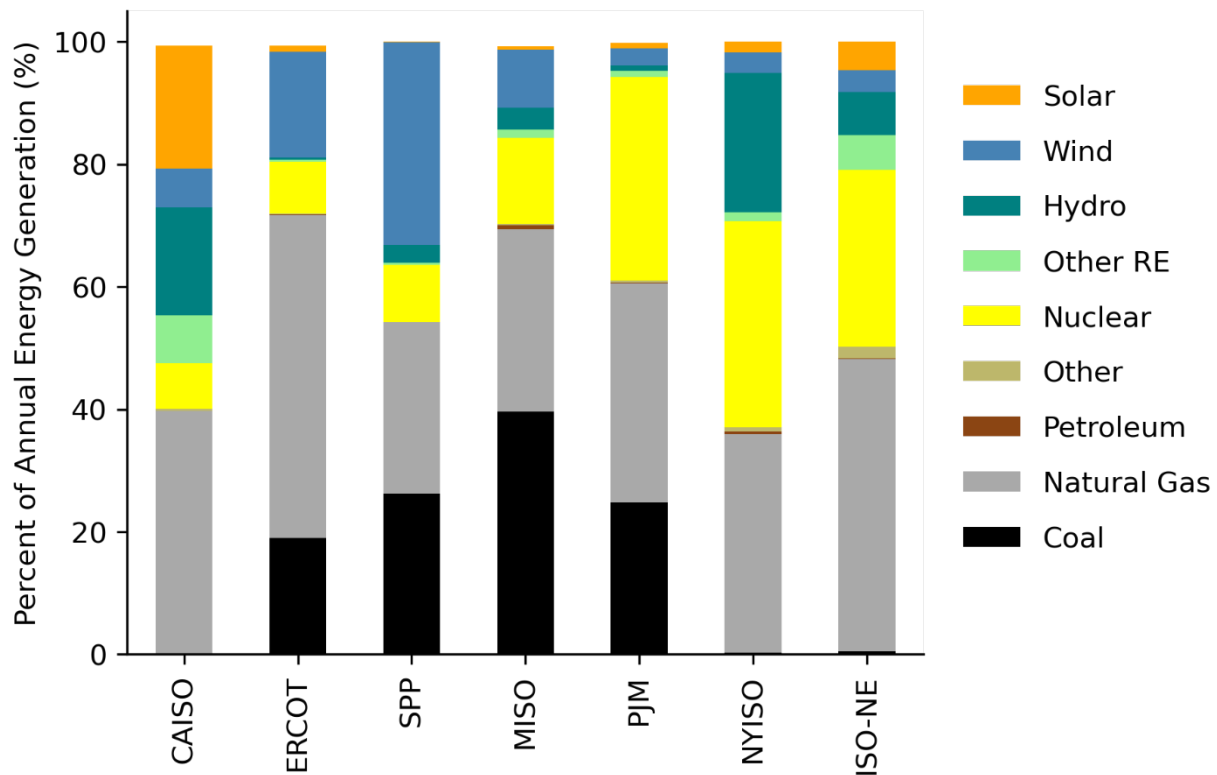
However, the grid planning studies have not yet incorporated coupled technologies into their frameworks, partly owing to the many possible configurations available, which make design of an internally consistent optimization program challenging [48]. A recent grid planning study by the Midcontinent Independent System Operator (MISO) compares the effectiveness of storage for increasing delivery of renewables to loads in scenarios targeting 40% renewables. The study finds that storage co-located with renewables enables greater delivery of renewables than storage located near loads. In addition, an algorithm designed to minimize transmission, storage, and production costs sited storage near renewables [49]. The scope of this study is limited in that the potential to deliver more renewable energy to loads is only one aspect of overall co-location impacts, and the study only covers one of seven U.S. market regions.

Because of model complexity, grid planning studies tend to limit the spatiotemporal granularity analyzed [50]. Though the internally consistent methods of capacity-expansion models allow comparisons across multiple generation resources, the limited spatiotemporal resolution limits the ability of these models to assess siting decisions involved with co-locating VRE and battery storage technologies. Furthermore, owing to the limited temporal resolution of these models, they struggle to realistically reflect volatility of energy prices and ancillary service prices.

We fill the research gaps by expanding on the system value studies, employing a broader market context that compares coupled renewable-battery projects to independent VRE and battery systems using historical wholesale market prices. Prior researchers have identified the key locational investment signals in modern electricity systems across the world. These signals include locational marginal prices (LMPs), grid connection and use fees, and capacity payments. We focus on LMPs and capacity payments, because they are the most significant geographic signals in many regions [51]. To understand the relative system value of VRE, battery, and coupled technologies, we rely on these geographically resolved market signals to generate system value metrics. Our research is possible because wholesale electricity markets in the United States (and in Australia and New Zealand) reflect the impact of transmission constraints and losses through LMPs defined at the nodal level. In contrast, only zonal prices are available in European markets, making it difficult to answer our research questions in those countries without detailed grid modeling [52]. Overall, our approach and geographic context allow us to incorporate detailed spatiotemporal variation in estimates of system value while comparing coupled and independent technologies in one consistent framework.

Because our analysis covers all seven U.S. organized wholesale markets, our findings are not limited to specific market conditions. The seven markets are diverse in their resource mixes and market characteristics (Figure 2-1). All seven markets operate a day-ahead and real-time energy market

with nodal LMPs that reflect transmission congestion. All markets similarly operate markets for ancillary services. In 2019, CAISO had the highest solar penetration at 18.7%; the New England Independent System Operator (ISO-NE) had the second highest at less than 5% [10]. Wind penetrations in 2019 were 27.5% in the Southwest Power Pool (SPP) and 19.9% in the Electric Reliability Council of Texas (ERCOT) [53]. CAISO is connected to the broader Western Interconnection and imports significant amounts of power. SPP, MISO, PJM Interconnection (PJM), the New York ISO (NYISO), and ISO-NE are all part of the Eastern Interconnection. ERCOT forms its own interconnection and has limited interconnection capability with neighboring markets. Load-serving entities in all the organized market regions except for ERCOT are subject to a mandatory resource adequacy requirement. CAISO and SPP rely on utility procurement or bilateral contracting to meet the resource adequacy requirement, while MISO, PJM, NYISO, and ISO-NE all operate forward capacity markets. Instead of a mandatory requirement, ERCOT’s “energy-only” market relies on the potential for high scarcity prices in the energy market to incentivize new capacity. As a result, prices have been most volatile in ERCOT, though constraints in the natural gas system have at times led to high volatility in CAISO, PJM, NYISO, and ISO-NE [10,54].



RE = renewable energy

Figure 2-1: 2019 Generation sources for ISOs in this study (Source: EIA [55,56])

3. Methods

Our methods section is split into four parts. First, we introduce the system value comparison framework developed to compare coupled projects to independent VRE and battery powerplants. This framework relies on two metrics that are used extensively in the results section. Next, we discuss how we calculate the corresponding system values for each technology, with a focus on our optimization formulation. The third section discusses the source of our main data inputs, and the last section outlines the scenarios we develop to check the robustness of our results.

3.1. COMPARISON FRAMEWORK

We apply a consistent approach to compare VRE generators, independent batteries, and coupled projects so we can investigate the drivers of regional differences in coupling development and identify the penalty associated with coupling. To do so, we develop two new metrics that evaluate the additional system value and additional constraints of coupled projects (i.e., reduced geographic options for battery siting, increased operational constraints due to infrastructure sharing, and restrictions on grid charging).

Our first metric, the “storage value adder,” aims to estimate the additional value of adding a battery to a renewable generator. This metric is calculated by subtracting the energy and capacity market value of the independent VRE generator from the energy and capacity market value of the coupled generator sited *at the same geographic location* as the VRE generator (Eq. 1).⁴ When estimating the storage value adder, developers will consider not only the value of coupled projects across markets, but also how coupled project value compares to alternative VRE investments. The storage value adder represents the additional revenue potential for a developer adding a battery project to a VRE generator.

$$\text{Storage value adder} = (E_{CP} + C_{CP}) - (E_{VRE} + C_{VRE}) \quad (\text{Eq. 1})$$

Where,

E = energy value of coupled project (CP) or wind/solar (VRE) systems in \$/MWh

C = capacity value of coupled project (CP) or wind/solar (VRE) systems in \$/MWh

This metric serves two purposes. First, by comparing this metric across different markets and years, we can evaluate how the value of adding batteries to VRE projects in certain regions changes over time, and how that value varies across regions. This result clarifies the potential for added storage to mitigate value deflation that occurs for a VRE generator in regions with high VRE penetrations. Second, we can directly compare this metric to the costs of storage and thereby assess the relative investment value of adding storage onto a VRE asset as discussed for a subset of markets in [24].

However, the storage value adder does not inform the coupling constraint of co-locating batteries at the same VRE location. We develop a second metric, the “coupling penalty,” to assess the relative

⁴ Ancillary service value is calculated in a sensitivity analysis discussed in Section 3.4.

value of independently siting storage technology. This metric is calculated by subtracting the market value of a coupled generator from the market value of an independent VRE generator and storage plant, *sited at different locations* (Eq. 2). Importantly, the coupled generator in this example uses the same VRE generator resource as the standalone VRE plant. There is only one key difference between the coupling penalty and the storage value adder. The coupling penalty includes new terms for the value of independently sited storage, and most importantly, the valuation of the storage system in this equation is not constrained by operational restrictions or co-location with the VRE generator. Instead, we choose a storage location based on identification of the most valuable storage nodes within a given market region, and we allow the storage to charge and discharge from the grid at its nameplate capacity. Therefore, this metric aims to quantify the coupling penalty associated with co-locating a battery and VRE resource at the same location and potentially introducing further operational constraints.

$$\text{Coupling penalty} = ([E_{VRE} + C_{VRE}] + [E_S + C_S]) - (E_{CP} + C_{CP}) \quad (\text{Eq. 2})$$

Where,

E = energy value of coupled project (CP), wind/solar (VRE), or storage (S) systems in \$/MWh

C = capacity value of coupled project (CP), wind/solar (VRE), or storage (S) systems in \$/MWh

Identifying valuable nodes is critical to our analysis, because it represents the key opportunity cost from siting a storage unit at a potentially less valuable nodal market location, to be near a VRE asset. Because we assume highly volatile nodes are the most valuable for storage as per the literature, we select the 30 most volatile nodes per market based on energy prices over the 2012–2019 period.⁵ For all energy pricing nodes in a particular year and market, we measure volatility as the standard deviation of prices.⁶ We focus on the top 30 nodes rather than the single most volatile node to test the sensitivity of our results to any individual high-value node. We then use the prices from those particular nodes to calculate the maximum standalone storage value using the optimization model discussed in the next section (in which the VRE resource, W_k , is 0 for all hours). Ultimately, we are interested in understanding whether the geographic constraint penalizes coupled projects, and that constraint will be driven by the potential revenue options available for batteries at these high nodal value locations.

⁵ Specifically, we calculate the volatility percentile for each of those nodes for each year, and we take the average percentile across all years. This averaging allows us to understand and limit our selection to nodes that are consistently volatile year-over-year rather than those that might be volatile for a limited period. This ensures a more stable storage value over typical storage asset lifetimes.

⁶ We select a set of nodes to study further based on standard deviation because it is cheaper to calculate than calculating the value of specific storage configurations.

3.2. SYSTEM VALUE ESTIMATION

We calculate two main system values for this research: (1) energy value, and (2) capacity value. A sensitivity analysis including the addition of ancillary services system value is discussed in Section 3.4.

The energy value is calculated by multiplying an hourly power generation profile by corresponding historical hourly real-time market prices (Eq. 3). The use of historical prices allows us to explore spatiotemporal variability not typically available in large-scale grid planning studies, as discussed in Section 2.

We use a simple and uniform approach for calculating the capacity value of independent and coupled resources, except in ERCOT. We do not calculate a capacity value in ERCOT because it is the only region where loads are not required to procure resources to maintain a planning reserve margin. In the other regions, we do not use region-specific capacity accreditation rules for coupled projects, because such rules are still under development [57]. Previous research indicates that average production during the peak net load hours can be a reasonable approximation of the reliability contribution of variable resources and coupled projects [39,58]. Hence, in this study, the capacity value is calculated by multiplying the same hourly power generation profile by a capacity price as well as an indicator variable for whether that particular hour of the year is within the top 100 net load hours for each specific market (Eq. 4). The capacity price is the annual average capacity price for each ISO, accounting for the capacity zone in all markets except SPP. Capacity prices from organized forward-capacity markets are used in MISO, PJM, NYISO, and ISO-NE. In CAISO, we use bilateral capacity prices for local resource adequacy as reported by the California Public Utilities Commission [59]. In SPP, we use the price of average short-term capacity transactions reported in Federal Energy Regulatory Commission (FERC) Electronic Quarterly Reports, which, relative to other sources of data, is more speculative [60].⁷ The use of an annual capacity price is a simplification, because capacity prices can vary by season, or even by month, depending on the market.

Eq. 3 and Eq. 4 correspond to variables in our framework equations from Section 3.1. Each of these values is estimated for independent VRE projects, independent battery projects, and coupled projects, and the underlying assumption is that operating these projects will not change wholesale prices (i.e., it is a “price taker” analysis). We normalize these values by the corresponding standalone VRE generation (G_{VRE}) in each case studied, including the standalone storage. We normalize the value calculations by generation to report metrics that are comparable to often-used cost metrics such as power-purchase agreement prices, bid prices in procurement, or levelized costs of electricity (LCOEs).

$$E_i = \frac{\sum_1^{8760} G_i * P_{rt}}{G_{VRE}} \quad (\text{Eq. 3})$$

⁷ We end up with high prices that might not be realizable in the actual market.

$$C_i = \frac{P_c/N \sum_1^{8760} G_i * NL_m}{G_{VRE}} \quad (\text{Eq. 4})$$

Where,

E_i = annual energy value of coupled project, VRE, or storage system in (\$/MWh)

G_i = hourly net electricity profile of coupled project, VRE, or storage system (MWh)

P_π = hourly real time electricity price (\$/MWh)

G_{VRE} = annual alternating-current (AC) generation output from the VRE generator (MWh)

C_i = annual capacity value of coupled project, VRE, or storage system (\$/MWh)

P_c = capacity price (\$/MW-yr)

NL_m = hourly indicator (0 or 1) for top N net-load hour for given market

N = number of top net-load hours, set to 100 in this analysis (h)

The electricity profile (G_i) for the standalone VRE asset is estimated via simulation (detailed in Section 3.3). In summary, we take latitude and longitude information for utility-scale solar and wind projects and simulate their hourly generation using weather data. These locations are then matched to the nearest nodal electricity market price (P_π). When prices are negative, we allow for curtailment of the standalone VRE electricity profile.

To estimate the electricity profile for the standalone storage asset, we develop a linear optimization model that maximizes wholesale market revenue by incorporating energy and capacity market prices. The full optimization model is described in Eqs. 5–11. The objective is to maximize net revenue, accounting for cycling-induced degradation (Eq. 5). The linear penalty on cycling the battery (D_p) aims to mirror the operational reality of deploying batteries in electricity markets.⁸ We take estimates of this parameter from the literature and run sensitivity analyses on its effect over the optimization results [61]. Constraints on battery operation are described by Eqs. 6–11.

The electricity profile for the coupled project relies on the same optimization algorithm as the standalone storage system, with three additional constraints (Eqs. 12–14). Eqs. 12 and 13 account for AC grid balancing when considering the addition of VRE generation. This constraint ensures that VRE production and battery charging/discharging match the energy output to the electric grid. Eq. 14 allows for curtailment when prices are negative and energy generation at the point of interconnection (POI) is unprofitable. The same renewable profile for the standalone VRE resource is used as an input to the coupled project optimization problem (G_{VRE}), and the creation of renewable profiles is discussed in greater detail in Section 3.3. The coupled project constraints below represent AC-coupled systems. Additional models that consider direct current (DC) coupled systems and ancillary service market products are described in Section 3.4 and the Supplementary Information.

⁸ In effect, this penalty sets the arbitrage value required to cycle the battery profitably. Our default assumptions limit cycling to arbitrage price differences greater than \$10/MWh, based on estimates from the literature.

We use the open-source optimization solver COIN-OR Linear Programming Interface [62]. The optimization model is implemented using the Julia programming language and the package JuMP [63].⁹

Objective function:

$$\text{Max } \sum_1^{8760} [(P_{rt} + P_c/N * NL_m) * G_i] - [D_p * (B_d + B_c)] \quad (\text{Eq. 5})$$

Subject to:

Beginning state of charge: $S_0 = 0$ (Eq. 6)

State of charge range: $0 \leq S_k \leq S_{max}$ (Eq. 7)

Power in rate: $0 \leq B_c(k) \leq B_{max}$ (Eq. 8)

Power out rate: $0 \leq B_d(k) \leq B_{max}$ (Eq. 9)

Non-simultaneity rule: $B_d(k) + B_c(k) \leq B_{max}$ (Eq. 10)

Battery state of charge: $S_{k+1} = S_k + \left[\eta B_c(k) - \frac{B_d(k)}{\eta} \right]$ (Eq. 11)

AC-grid limits: $-I_g B_{max} \leq G_i(k) \leq POI$ (Eq. 12)

AC-grid balance: $G_i(k) = W(k) + B_d(k) - B_c(k)$ (Eq. 13)

Curtailement allowance: $W(k) \leq G_{VRE}(k)$ (Eq. 14)

Where the decision variables are,

G_i = hourly net electricity profile of coupled or storage system (MWh)¹⁰

B_d = battery discharging (MWh)

B_c = battery charging (MWh)

S_k = battery state of charge at time step k (MWh)

W_k = power generated from renewable resource at time step k

⁹ Owing to the wide parameter space, which encompasses more than 500,000 unique optimization runs, we also implement an embarrassingly parallel program on Lawrence Berkeley National Laboratory's Lawrence Livermore high-performance computer to speed up the development of results.

¹⁰ For battery systems, this is more explicitly written as $B_d - B_c$.

Where the input parameters are,

P_{rt} = hourly real time electricity (\$/MWh)

P_c = capacity price (\$/MW)

NL_m = hourly indicator (0 or 1) for top N net-load hour for given market

N = number of top net-load hours, set to 100 in this analysis (h)

D_p = degradation penalty (\$/MWh)

B_{max} = battery max power capacity (MW)

S_{max} = total energy capacity of battery (MWh)

η = battery one-way efficiency (%)

I_g = binary indicator to allow grid charging (1 allows grid charging, 0 restricts charging to available VRE)

POI = point of interconnection limit

G_{VRE} = standalone VRE generation profile

We apply the optimization program using two distinct algorithms to develop an optimistic and pessimistic market value estimate for both independent storage projects and coupled projects. Our optimistic algorithm assumes perfect foresight of real-time electricity prices and VRE generation profiles when determining optimal dispatch (perfect foresight method). Conversely, our pessimistic algorithm generates an optimal dispatch schedule based on day-ahead prices and the prior day's VRE profile as a forecast of today's profile. The realized revenue is then calculated by applying this "day-ahead" dispatch schedule to real-time market prices (day-ahead schedule method). In the day-ahead schedule method, the realized battery charge and discharge schedule is adjusted by constraining the optimized schedule with the operating day's actual VRE generation profile as well as limits on the coupled battery in a post-process calculation detailed in the Supplementary Information.

3.3. DATA COLLECTION

Our analysis has three key hourly data inputs: (1) VRE generation profiles, (2) location-based market prices, and (3) net-load profiles. Each of these data inputs is collected for the 2012–2019 period and for the seven main U.S. ISOs (CAISO, ERCOT, MISO, SPP, PJM, NYISO, and ISO-NE).

To produce generation profiles, we first collect weather data at the main U.S. utility-scale PV and wind locations identified by U.S. Energy Information Administration (EIA) Form 860 for the ISOs indicated above [64]. This process results in 2,117 unique PV and 617 unique wind locations. We consider only existing locations rather than all potential locations to ensure that our analysis only considers sites with a proven resource and ability to site a utility-scale plant.

We download solar irradiance data from the National Renewable Energy Laboratory's (NREL's) National Solar Radiation Data Base using the corresponding latitude and longitude information from EIA [65]. To create the solar generation profiles for a single-axis tracking plant, we use NREL's System Advisor Model (SAM), which outputs both AC—which passes PV panel production through an inverter—and DC solar production profiles [66]. For these simulations, we use default system losses of 14% and an inverter efficiency of 96%.

We develop wind power estimates at existing wind plants using the average 2018 power curve for installed U.S. wind plants [67]. We rely on weather data from the reanalysis product ERA5 [68]. ERA5 is produced by the European Centre for Medium-Range Weather Forecasts. ERA5 currently provides data for 1979 to the present and has a horizontal resolution of roughly 30 km. To use the ERA5 data, we first remove long-term bias in the ERA5 wind speeds for individual plants. To debias wind speeds, we use generation records from the first 2–5 years of existing wind plants to find the implied average wind speed from the recorded generation, and then we scale ERA5 wind speeds to match this implied average wind speed. We then apply these scaled ERA5 wind speed time series to our common power curve. Further details on the scaling process can be found in the Supplementary Information.

We collect hourly real-time and day-ahead LMPs and regulation market prices for all seven U.S. ISOs from ABB’s Velocity Suite data product (covering 52,307 nodal prices) [69]. Most wind or solar plants are assigned to a corresponding LMP node within the ABB product. For plants not assigned to a node, we use a nearest-neighbor algorithm to identify the closest match for a specific year.

Table 3-1 displays the count of locations run through our optimization program by ISO and location type. A number of the wind and solar plants collected by EIA are small and thus not likely applicable to utility-scale coupled projects. In our results, we only consider solar and wind plant locations with powerplant sizes greater than 5 MW-AC, to avoid concerns that some smaller generators would not be suitable locations for utility-scale plants. The high-volatility nodes are selected with three filters: (1) must exist for all years in sample (2012–2019), (2) are in the top 20th percentile of volatility for a given market, and (3) are at least 10 km away from each other. From this filtered list, we select the most volatile node and 30th most volatile node for analysis as discussed in Section 3.1.

ISO	Solar	Wind	High Volatility
CAISO	226	48	43
ERCOT	51	97	84
ISO-NE	75	19	38
PJM	212	58	132
MISO	120	156	35
SPP	19	116	175
NYISO	21	21	17
Total	724	515	524

Table 3-1: Count of locations modeled by market and generation type after filtering for solar and wind sites larger than 5 MW-AC

Finally, we collect hourly net load data for each market. Net load is the ISO/RTO-reported load less the system-wide aggregate solar and wind generation profile, which is also from the ABB Velocity Suite. Our capacity cost is then evenly allocated across the top 100 net load hours of the

year. After collecting these three different data types, we combine them into hourly time series to be used as the main inputs to the optimization formulation discussed above.

3.4. ROBUSTNESS AND SENSITIVITIES

Our key modeling parameters and their corresponding default and sensitivity assumptions are summarized in Table 3-2. The first three assumptions represent the three key coupling constraints we model: (1) increased operational constraints due to infrastructure sharing, (2) restrictions on grid charging,¹¹ and (3) reduced geographic options for battery siting. Our default assumptions are set to explore the uppermost end for the coupling penalty. We individually adjust these default assumptions to understand how each contributes to limitations on coupling value. Assumptions 4–7 represent the subset of input parameters we adjust to test the robustness of our results.

We maintain a wide sweep of geographic locations (1,763 nodes) and historical years (5 total). To reduce the scale of the parameter space, we do not adjust the storage size and duration. Rather, we base the assumptions for those two parameters on coupled projects currently in the commercial development pipeline, as described in prior work [21,24,70]. We ensure the relative AC-based generator and battery sizes match between our coupled and standalone VRE/battery configurations.

Parameter	Default value	Sensitivity analysis values
1. Interconnection limit (MW) ¹²	VRE capacity	VRE + battery capacity
2. Grid charging	Disallow grid charging	Allow grid charging
3. Independent battery node	Most volatile in given market over 8-yr period	30 th most volatile in given market over 8-yr period
4. Dispatch algorithm	Perfect foresight	Day-ahead schedule
5. Degradation penalty	\$5/MWh	\$25/MWh

¹¹ This assumption affects the ability of a wind or solar plant to qualify for the investment tax credit (ITC), which requires 75% of a battery’s energy to come from renewable energy for the first 5 years of operation. The production tax credit (PTC), typically used by wind plants (in lieu of an ITC), cannot be applied to storage. Coupled wind-battery plants that take the PTC would, as a result, not be constrained to charge from the wind plant. However, wind plants can and sometimes have taken the ITC, in which case such plants would seek to charge solely or primarily from the wind facility.

¹² The limit is driven by the capacity at the POI requested by the developer from a transmission operator. This is a developer choice, rather than a fixed constraint, which is why we perform a sensitivity analysis where we increase the POI limit to the maximum capacity of the VRE plus the battery device.

6. Ancillary services	Exclude regulation value	Include regulation value
7. Solar ILR and coupling	1.3 AC-coupled	1.7 DC-coupled
8. Wind coupling	AC-coupled	N/A
9. VRE size (MW _{AC})	100	N/A
10. Storage size (%)	50% of generator capacity	N/A
11. Storage duration (hr)	4	N/A
12. Geographic	1,763 pricing nodes	N/A
13. Years	2012, 2014, 2015, 2017, 2019	N/A

Table 3-2: Modeling parameter choices

In addition to testing the sensitivity of our results across these parameters, we develop two alternative models to further gauge the robustness of our results. The first alternative model considers ancillary service markets. We restrict this modeling to only consider the system value in regulation reserve markets, rather than other ancillary service markets, owing to their relatively high prices [71]. The regulation reserve system value is calculated by multiplying a regulation reserve schedule by hourly regulation reserve prices (Eq. 15). Regulation reserve prices are often aggregated at the market level with limited geographic differentiation. CAISO is an exception. Therefore, we assign each non-CAISO plant in our sample to its corresponding market regulation price, while CAISO plants get assigned to their closest ancillary service zone. This system value is then added to the corresponding energy and capacity values estimated via Eqs. 1 and 2 (Section 3.1) for coupled projects and independently sited storage.

We assume independent VRE projects cannot provide ancillary service value, because they typically do not participate in those markets in the United States [71]. To generate the regulation reserve profile (R_i), we use the same basic optimization algorithms discussed above but add additional constraints and terms to the objective function. These additions are detailed in the Supplementary Information.

$$AS_i = \frac{\sum_1^{8760} R_i * P_{as}}{G_{VRE}} \quad (\text{Eq. 15})$$

Where,

AS_i = annual ancillary service value of coupled or storage system (\$)

R_i = hourly regulation reserve profile of coupled or storage system (MWh)

P_{as} = hourly regulation reserve price (\$/MWh)

G_{VRE} = annual AC generation output from VRE generator (MWh)

The second alternative model we implement is a DC-coupled solar-battery plant with an inverter loading ratio (ILR) of 1.7. Though AC-coupled systems remain the most popular configuration, there is interest in DC-coupled systems owing to their ability to capture energy typically clipped by solar inverters [72]. To model these systems, we simulate the DC output for our solar nodes using NREL's SAM without incorporating AC inverter losses. We pass this augmented generation profile into an updated optimization algorithm that explicitly models the DC-to-AC conversions between the PV system, battery, and grid. The equations used for the DC optimization model are detailed in the Supplementary Information. System value results from the DC-coupled model are used to determine whether our geographic trends across time are robust. Comparisons on an absolute basis to the default case and other sensitivities must be done cautiously, because the full comparison would need to consider construction costs, given the larger panels and energy production in the DC case.

4. Results

We present our results in two sections, each focused on the different evaluation metrics discussed in Section 3.1. The first section focuses on the storage value adder, a key indicator of the market drivers towards coupling. The second section concentrates on the coupling constraints, a potential limitation of these project types.

4.1. ESTIMATES OF THE STORAGE VALUE ADDER

The value boost of adding storage to a VRE plant ranges from \$3–\$22/MWh depending on the year and region, with an average value of \$10/MWh. In 2019, the benefit of adding storage to a wind or solar plant in CAISO or ERCOT, as measured by the storage value adder, is \$13–\$21/MWh. This figure is 50%–340% higher than the benefit of adding storage to wind or solar in the other ISOs (Figure 4-1). ERCOT's high storage value adder, however, is limited to 2019, a year with frequent scarcity prices topping \$9,000/MWh during summer peak periods [73]. The relatively high value adder in CAISO after 2015 aligns with changes in that region's pricing patterns. Increased solar penetration made prices low when the sun is out and high when it sets, enabling valuable storage arbitrage. CAISO's higher adder for solar, in particular, shows how coupled batteries partially offset the solar value decline resulting from these pricing changes. This result accords with the popularity of coupled solar projects over coupled wind projects (Table 1-1). In addition, the grid charging and POI constraint become less binding as higher solar penetration levels push high electricity prices outside of solar hours.

As context, past research estimated that adding 4-hour batteries sized to 50% of the nameplate capacity of a PV plant, comparable to the PV configuration studied here, increases cost by \$10/MWh [24]. This cost increase is lower than the storage value adder calculated in our default case in many regions and notably lower for each year modeled in CAISO. Future battery cost reductions are expected [74], which would make coupled-system economics more attractive.

In most cases, the relative difference of the storage value adder across ISOs does not strongly depend on whether storage is coupled with solar or wind. Though the magnitude of the storage value adder for solar averages \$2.4/MWh higher than for wind, these differences are partially driven by the larger capacity factors for wind, which result in lower levelized energy values rather than storage values in particular. This divergence, however, is more pronounced in CAISO, where the storage value adder for solar exceeds the adder for wind by \$6–\$8/MWh in 2017 and 2019, surpassing differences resulting from capacity factor effects alone. The steady increase in storage value for solar in CAISO correlates with a rise in solar penetration from 2% in 2012 to 19% in 2019 [10]. Over the same period, the storage value adder for wind in CAISO remains relatively constant. Restrictions on POI can particularly affect solar coupling owing to greater alignment of solar production and peak periods with high prices.

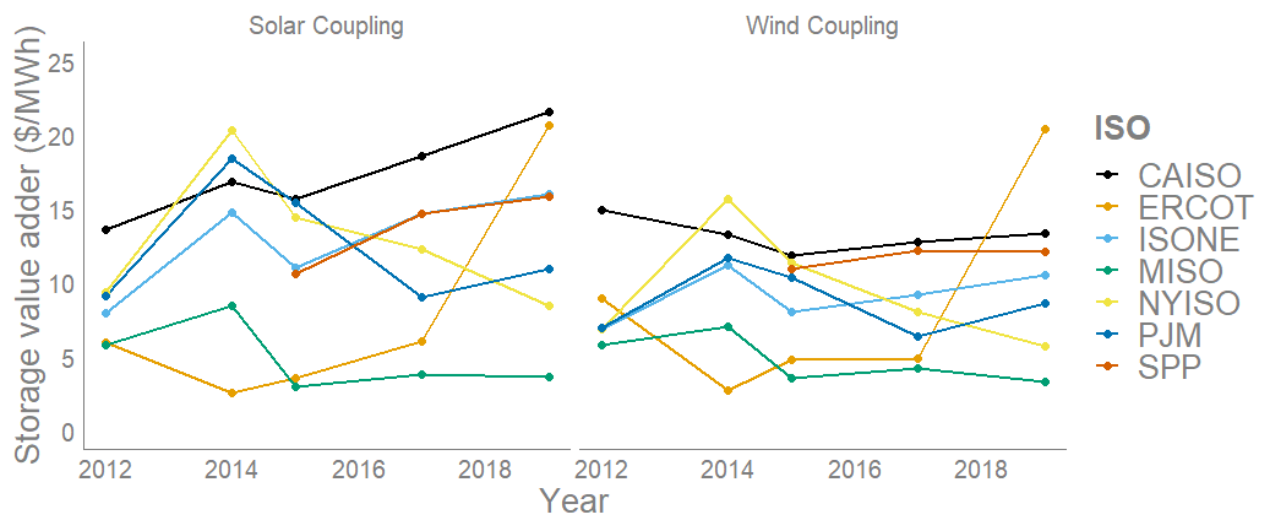


Figure 4-1: Average storage value adder for solar and wind coupled projects by market assuming perfect foresight, showing high value for CAISO region

Figure 4-2 breaks out the two components of the storage value adder: (1) coupled project value, and (2) VRE generation value. The benefit of adding storage to solar makes up for the decline in solar market value in CAISO between 2012 and 2019 (Figure 4-2, top left). Conversely, the value of wind in CAISO increases between 2012 and 2019 (Figure 4-2, top right). Thus, adding storage further increases, rather than just maintains, the value of the wind coupled projects from 2012 to 2019 in CAISO, but there is not a corresponding increase in the storage value adder. For ERCOT, there is no value decline for wind or solar in the same period, and both types of coupled projects see value increases in 2019 with the rise in scarcity prices. This increase in coupled value outpaces the rise of the VRE asset value, leading to increases in the storage value adder.

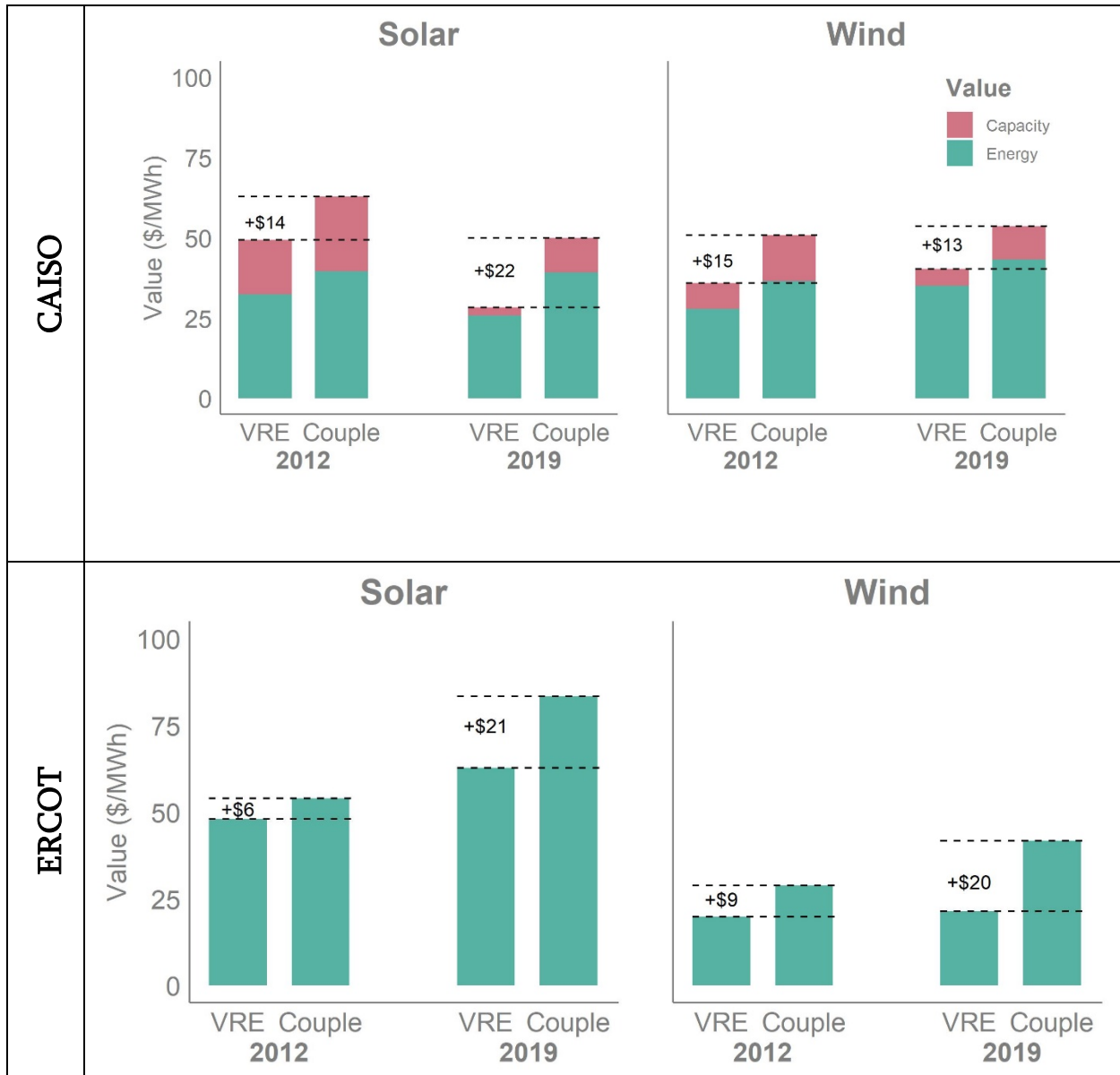


Figure 4-2: Average VRE and coupled values in CAISO and ERCOT, showing different storage value adders between 2012 and 2019 (black text)

We find some divergence from these aggregated market results when assessing this metric at individual node locations. Figure 4-3 plots the difference between the storage value adder and the *average* storage value adder within a given market at all the wind and solar nodes in our sample. For instance, California solar along the Mexican border has a storage value adder about \$4/MWh above average (i.e., a \$26/MWh storage value adder in 2019). These plots suggest that our results have limited variation at the nodal level within a market. This result highlights the fact that regional wholesale pricing trends *across* markets are more important than differences brought about by historical transmission constraints *within* the markets. ERCOT is a notable exception,

where a few nodes in the western portion of Texas see substantially higher values than the ERCOT market average, suggesting extreme nodal variation.

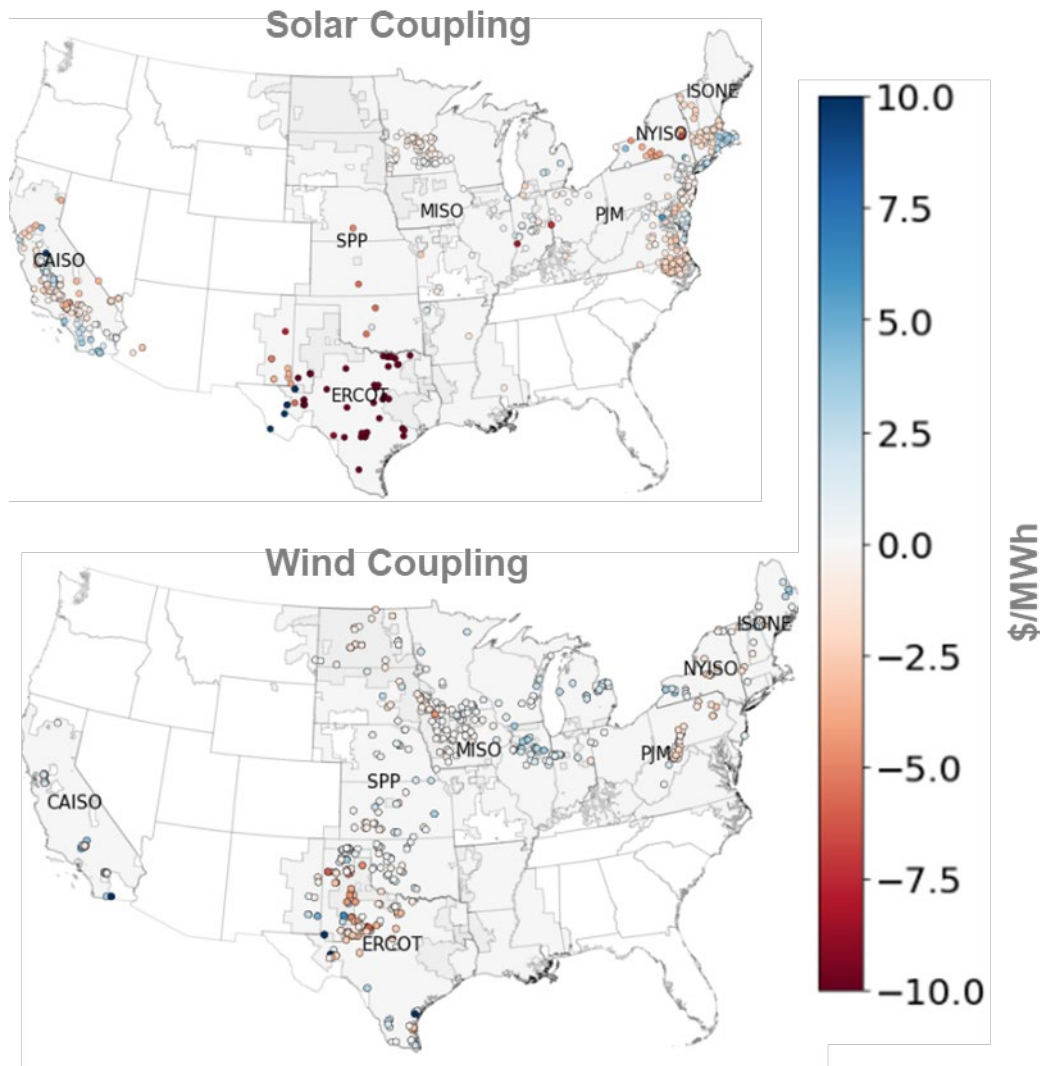


Figure 4-3: Geographic variation in storage value adder relative to the market average storage value adder for solar and wind coupled projects in 2019. Extreme values in ERCOT range to \$52/MWh for solar and \$91/MWh for wind but are reduced to limit the color scale.

The relatively high storage value adders in CAISO and ERCOT and the similar magnitude of the storage value adder for wind and solar in most ISOs are found across a wide range of sensitivity cases (see the Supplementary Information). Increasing the assumed degradation penalty from \$5/MWh to \$25/MWh consistently reduces all storage value adders by \$1–\$3/MWh. Across most years and ISOs, allowing grid charging and increasing the POI limit increases the storage value adders by \$2–\$18/MWh for solar and \$1–\$6/MWh for wind, with the biggest changes in ERCOT as described below. Changing the solar coupling to a 1.7-ILR DC-coupled system maintains the same trends across ISOs and years, except the storage value adder is \$6/MWh lower in ERCOT in

2019 owing to the revenue from generation during scarcity hours being spread over a larger annual generation level.¹³ The day-ahead schedule algorithm, which schedules the battery using day-ahead rather than real-time prices, decreases the storage adder for wind and solar coupled projects by \$2–\$11/MWh, with negligible changes in the relative magnitude of solar’s storage value adder over wind’s.

Only one sensitivity case significantly changes the finding that storage adders are highest for CAISO relative to other regions. When the coupled project provides regulation reserve services, the storage value adder increases by \$5–\$55/MWh above the default case. This boost is particularly high for PJM in 2014, and the storage value adder in ISO-NE surpasses the adder in CAISO for 2015–2017, suggesting particularly lucrative ancillary service markets in those regions.

However, regulating reserve requirements are relatively small. The requirement in ISO-NE in particular (60 MW) is too small to benefit large penetrations of coupled renewable-battery projects and storage technologies [71]. Across all seven ISOs, the demand for regulating reserves is 2–6 GW. The battery storage proposed in those markets is an order of magnitude greater, potentially leading to a situation in which the regulating reserves supply will swamp demand and thus depress prices for these services [24]. In such a scenario, we would expect the large effect of this sensitivity case on our results to drop significantly.

Allowing grid charging and relaxing the shared POI constraint have interesting effects in CAISO and ERCOT. In CAISO, the storage value adder increases by \$10/MWh in 2012 compared to a smaller increase of \$3/MWh in 2019 when removing the constraints (see the Supplemental Information). The effect is even more noticeable in ERCOT, where relaxing these constraints increases the 2019 storage value adder for solar in ERCOT by \$20/MWh compared to only \$5/MWh on average for the other years studied.

Prior research has shown that in CAISO in 2012, solar generation aligned with periods of high prices, and by 2019 high-price periods shifted to early evening after sunset while low prices shifted to the middle of the day [10]. Under these pricing conditions, there is less opportunity cost associated with charging from solar in the middle of the day in 2019 as compared to 2012. Limiting the POI capacity to the VRE AC capacity is less binding in 2019, because storage can fully discharge during high net-load periods after sunset. A similar result occurs in ERCOT in 2019, where the POI and grid charging constraints limit the coupled project’s opportunity to discharge during scarcity events. Both these results indicate that storage and solar would ideally both provide power to the grid during the afternoon scarcity price events, though this constraint is less important if high prices are not aligned with solar or wind production.

¹³ This effect is unique to ERCOT because of the very high scarcity prices concentrated in a limited set of hours that happen to align with peak solar hours, where the maximum capacity of the coupled system is limited by the POI constraint rather than energy limitation.

4.2. QUANTIFYING THE COUPLING PENALTY

Section 4.1 focuses on the additional value from adding storage to VRE. This section quantifies a potential drawback by considering the three coupling constraints of co-location: (1) geographic restrictions on battery siting, (2) limitations on shared infrastructure capacity, and (3) restrictions on grid charging. To do so, we compare the value of a coupled project with the value of the same equipment (VRE and batteries) sited independently.

We find that the coupling constraint is significant using our default assumptions. The value of independently sited VRE and storage exceeds the value of coupled projects in all markets and years, except for wind in ERCOT in 2012 (Figure 4-4). Across most markets and years, the coupling penalty is \$2–\$50/MWh, averaging \$12.5/MWh. These results are sensitive to the POI and grid charging assumptions, which are distinct from the geographic siting constraint. When relaxing these two constraints, this penalty drops by \$5/MWh on average (see the Supplementary Information).

There is a particularly high coupling penalty (\$30–\$50/MWh) for NYISO between 2012 and 2015 owing to the particularly high value for independently sited storage in NYISO’s Long Island region during these years. Aligned with this finding, 98% of proposed batteries are to be sited independently from VRE in NYISO’s interconnection queues [21]. In SPP and ERCOT, 62% and 63% of proposed batteries, respectively, are to be sited independently from VRE, compared with only 36% in CAISO.

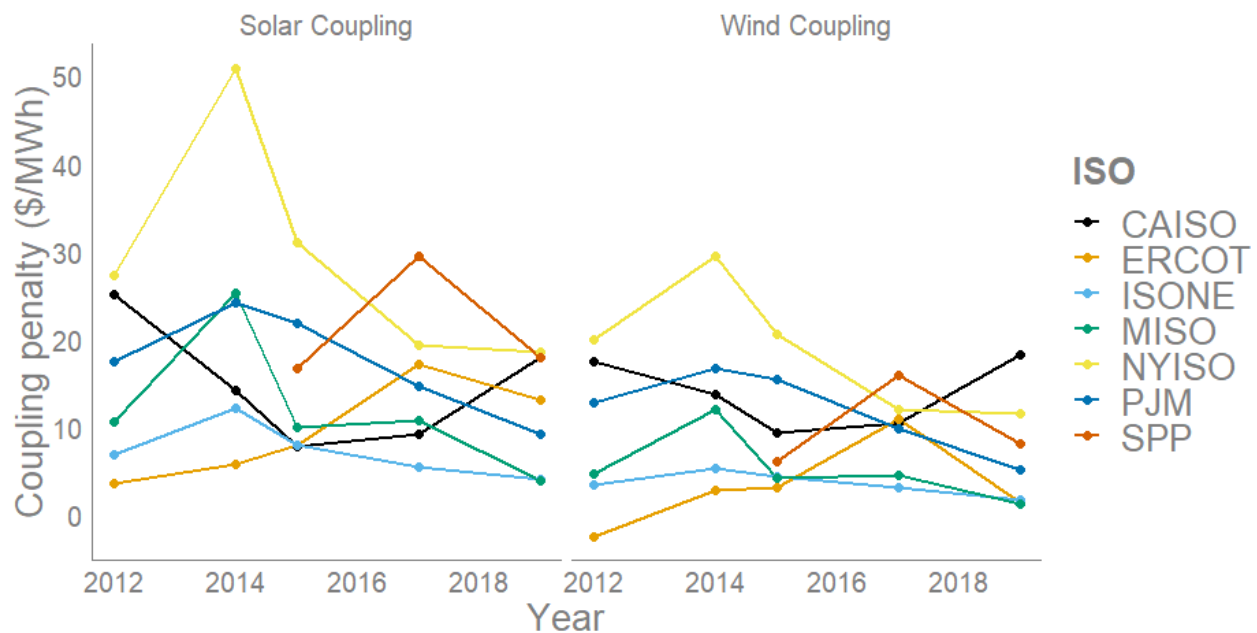


Figure 4-4: Average coupling penalty for solar and wind projects by market assuming perfect foresight, showing consistently positive penalty values

The positive coupling penalty across markets and years suggests that storage value at our selected high-volatility node is higher than the value of storage at solar and wind nodes (Figure 4-5). On the other hand, regions with similar value between node types do not have a significant coupling penalty from co-location. ISO-NE in particular shows very little deviation between solar, wind, and high-volatility node storage values. This result corresponds to the relatively negligible coupling penalty in Figure 4-4 for ISO-NE. ERCOT has the most storage value spread among these market regions, but the differentiation between node types is still limited, especially at the extreme end of the distribution. Though we could not calculate storage value across all 50,000-plus nodes in our seven market regions owing to computational limitations, we calculate the corresponding standard deviations for all nodes (see the Supplementary Information).

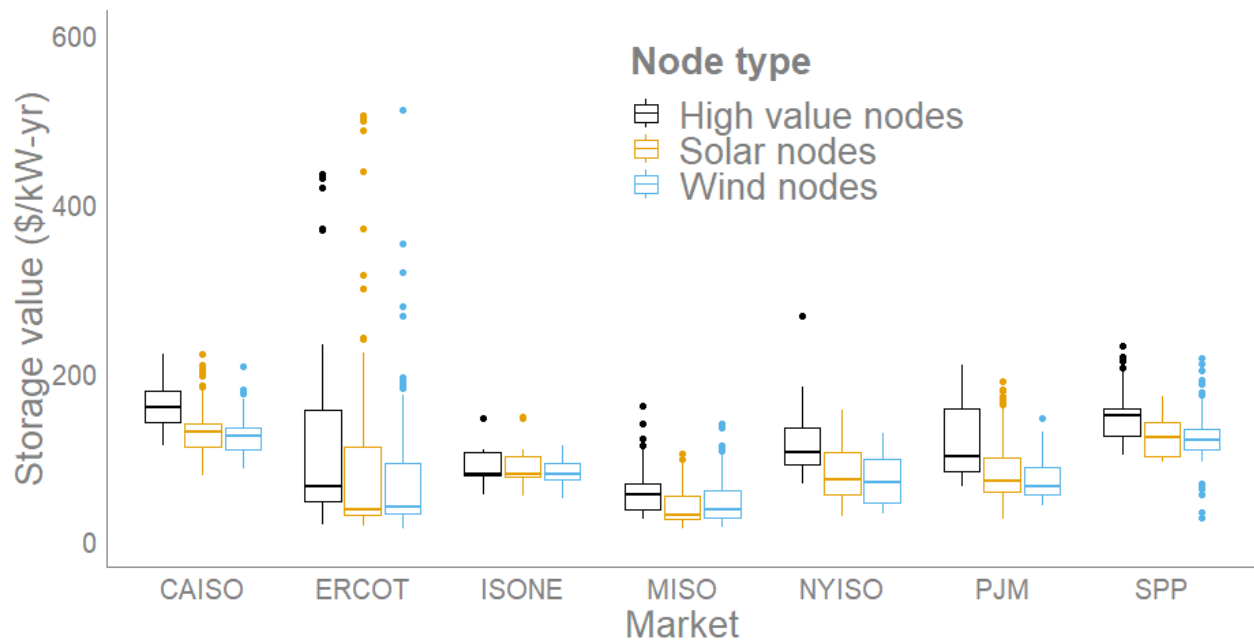


Figure 4-5: Annual standalone storage value across different node types and by market for each year between 2012 and 2019

While the median storage value at high-volatility nodes is higher than the corresponding median value at wind and solar nodes, there is significant overlap in the distributions. As a result, the high-value nodes do not always result in higher storage value compared to individual wind and solar nodes in specific years (Figure 4-5). In some cases, deploying storage at a VRE location in a coupled configuration could be more valuable than independently sited VRE and storage. Still, only 1.5% of utility-scale wind and solar locations in our sample have negative values for the coupling penalty in our default case.

Figure 4-6 plots the coupled project value on the x-axis and the sum of the independently sited VRE and storage value on the y-axis. The dashed gray line represents a coupling penalty of \$0/MWh. Symbols to the left of the line represent a positive coupling penalty (independent system

more valuable), and symbols on the right represent a negative coupling penalty (coupled system more valuable). The negative coupling penalties are most common in ERCOT.

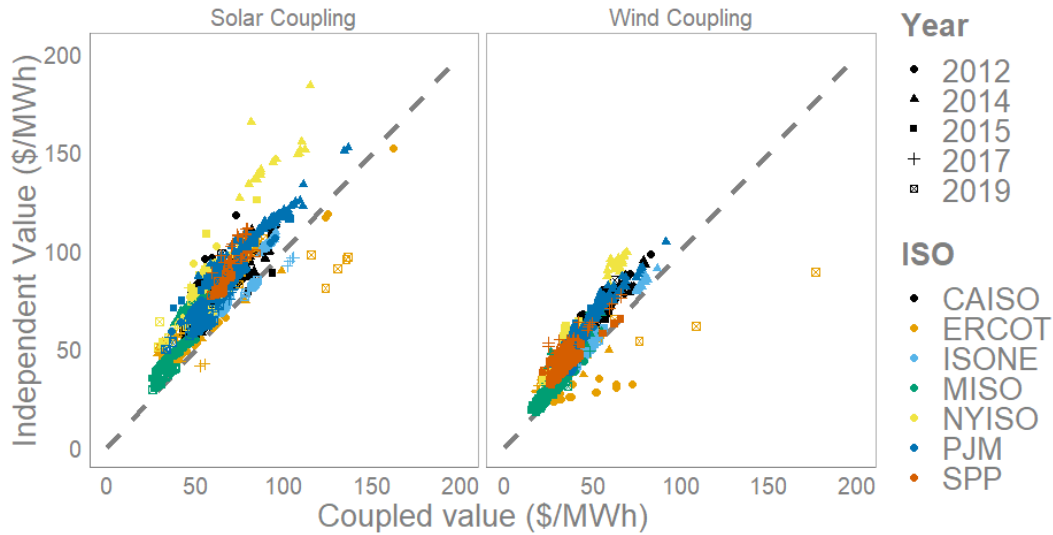
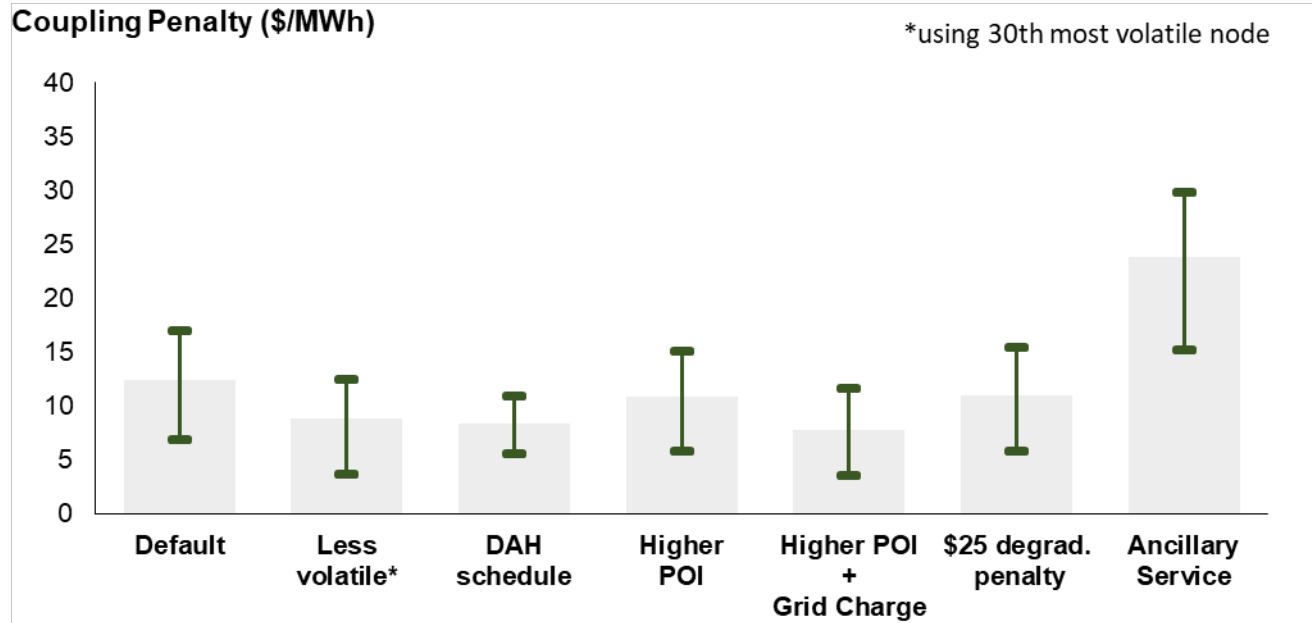


Figure 4-6: Comparison of coupled project value to standalone value for all wind and solar nodes

The predominantly positive value for the coupling penalty is robust to the sensitivity cases (see the Supplementary Information), but the magnitude of the penalty is substantially reduced in a number of them. Applying the lower-volatility, day-ahead schedule, or relaxed grid charging and POI constraint cases reduces the magnitude of the average penalty by \$4/MWh, \$4/MWh, and \$5/MWh, respectively (Figure 4-7). A combined case incorporating each sensitivity case into one case results in a coupling penalty of only \$1.6/MWh on average. The ancillary service case, on the other hand, increases the coupling penalty by an additional \$11/MWh.



DAH = day-ahead

Figure 4-7: Average coupling penalty across all nodes and years. Ranges represent 80th to 20th percentiles of coupling penalty.

5. Discussion

The results above quantify the potential value of coupling wind or solar with storage, and they show the potential loss in value due to coupling the VRE and storage together rather than seeking to maximize value by siting each resource independently. However, they do not show the difference in cost between coupled and independently sited resources. The economic attractiveness of coupling depends on whether the cost savings from coupling outweigh the value penalties.

Figure 5-1 compares our detailed coupling penalty estimates with a rough estimate of potential cost savings from coupling. It shows the average default coupling penalty, \$12.5/MWh, as well as penalty reductions due to conditions in our sensitivity cases, which together reduce the penalty to \$1.6/MWh. In contrast, the potential cost savings from coupling are around \$15/MWh—outweighing our estimated coupling penalties, even in the default case, and making coupled project development more attractive than independent siting of battery and VRE technologies on average.

There are reasons to believe that real-world penalties will tend to be lower than the default-case penalty as depicted in Figure 5-1. On average, about \$5/MWh of the default penalty results from the grid charging and POI constraints. Though these constraints appear to be common today [24], they are developer decisions. Siting independent battery systems at less-volatile (lower-value) nodes offers around \$4/MWh in penalty reduction. For our default case, we identify and site batteries at high-volatility nodes using historical data. However, predicting future high-volatility locations is challenging; the highest-volatility nodes could become saturated with storage, and the

prevalence of less-volatile nodes in a region likely make them a more realistic, long-term target for battery siting. Finally, assuming a dispatch algorithm with a day-ahead schedule rather than perfect foresight is also more realistic and could reduce the coupling penalty by another \$3/MWh.

The potential cost savings from coupling in Figure 5-1 entail more uncertainty. Researchers have indicated that construction cost synergies for coupled PV-battery projects could reduce total costs by 7%–8% compared with the costs of independent PV and battery projects [75]. These studies rely on bottom-up engineering estimates, and these modeled savings may be higher or lower in reality. Assuming these percentage reductions hold, the savings from coupling could be equivalent to roughly \$5/MWh, of the same order of magnitude as the coupling penalties we calculate in our default and sensitivity cases.¹⁴ The ITC could add another roughly \$10/MWh to the cost savings from coupling, if the battery charges exclusively from the VRE.¹⁵ The ITC will step down from 30% (for projects that began construction by 2019) to 10% (for projects beginning construction in 2022). Though ITC project cost savings are solely a financial transfer to developers rather than a way to minimize system costs, they still incentivize coupling. Even if the ITC were to be eliminated, commercial interest in coupled projects would likely remain due to construction cost synergies exceeding the magnitude of coupling penalties in many regions.

¹⁴ We calculate LCOE (\$/MWh) cost savings using benchmark coupled PV-storage power-purchase agreement data reported in [70]. The resulting assumptions are: (1) 100-MW, 1.3-ILR PV system with a 30-year lifetime and 26% capacity factor at \$1,414/kW-AC, (2) 50-MW, 4-hour storage system with a 15-year lifetime at \$400/kWh. The coupling benefit is calculated by multiplying 7% by the LCOE of the combined PV-storage system.

¹⁵ The ITC benefit is calculated by multiplying the storage-only LCOE by 30%.

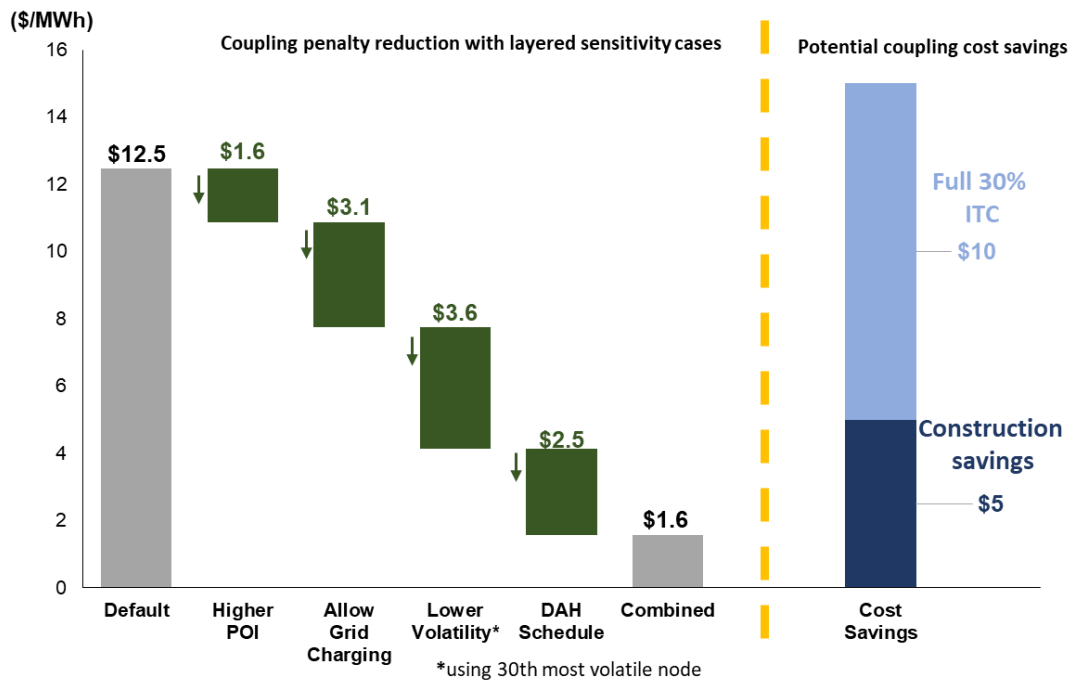


Figure 5-1: Comparison of the coupling penalty across the combination of sensitivity cases with the potential cost incentives resulting from coupling

6. Conclusions and Open Research Questions

We draw several conclusions from this study. First, the recent commercial interest in coupled renewable-battery projects broadly accords with our regional estimates of storage value adders. This is most apparent for CAISO, which averaged the highest default-case storage value adders between 2012 and 2019 as well as the highest percentage of proposed renewable-battery coupling at the end of 2020. CAISO’s higher adder for solar, in particular, shows how coupled batteries partially offset the solar value decline resulting from the region’s electricity pricing changes driven by increasing solar penetrations. As other regions increasingly install solar, they may demonstrate greater interest in solar-battery projects as well.

At the same time, the default-case coupling penalty is significant across most markets and years, averaging \$12.5/MWh or a 21% reduction in the value of independently sited VRE and storage. This penalty is, in part, due to geographic restrictions on battery siting. Past considerations for solar and wind siting decisions were often limited to resource potential, transmission access, market value, and land availability [76,77]. The coupling penalty suggests that adding nodal volatility to the list of considerations may become increasingly important in a future with higher development of battery and coupled technologies.

However, the default-case case penalties were also driven by limitations on shared infrastructure capacity and restrictions on grid charging, and there are reasons to believe that real-world coupling penalties will tend to be lower than these default-case penalties. Based on our sensitivity cases,

easing the grid charging and POI constraints, which are developer decisions, reduces the default-case coupling penalty by about \$5/MWh. Developers will continue to learn from deployment experience, and they will optimize system design and operation decisions to mitigate the impact of these constraints. Combining the developer-driven reductions with a day-ahead (rather than perfect foresight) dispatch algorithm and lower-volatility (lower-value) siting of independent battery systems brings the average penalty to only \$1.6/MWh (3% reduction in the value of independently sited VRE and storage). This result implies limited divergence in storage arbitrage value across pricing nodes within a given market, resulting in little opportunity cost to geographic co-location.

Finally, we roughly estimate potential costs savings from coupling at around \$15/MWh, including construction costs savings and use of the ITC—outweighing our estimated coupling penalties, even in the default case, and making coupled project development more attractive than independent siting of battery and VRE technologies on average. However, the wide regional variation in coupling penalties, along with the importance of conditions captured in our sensitivity cases, suggests the tradeoff between coupling penalties and savings will vary by situation. Therefore, roles exist for independent and coupled projects from a system optimization perspective, which is also consistent with the commercial interest in coupled renewable-battery projects. Furthermore, we do not address other system values not currently priced in wholesale markets, such as the benefits of mitigating dynamic stability issues in weak grids, but, as shown in a detailed grid-modeling assessment, these can be another important reason to site storage near renewables [49].

As storage technologies continue to develop, there remain many open research questions. First, there is a need to understand how our results might change under high VRE and storage penetrations [78]. For instance, ancillary service markets are small today but could become increasingly important as VRE growth increases the need for ancillary service products. Furthermore, there is interaction among VRE and storage penetration and the ultimate size of the energy arbitrage potential, which is a challenge we did not address with our price-taker formulation. Estimating the depth of arbitrage opportunity remains an important open question for both independent and coupled battery development. Beyond ancillary service markets, coupled projects may have other hard-to-quantify option values associated with being able to adapt the operating strategy to fit evolving grid needs.

Second, researchers should investigate the most cost-effective coupled configurations. When developers make coupling design decisions—decisions that depend on absolute rather than relative system value—they will choose between configurations beyond those we model here, considering market prices and construction costs. We focus on today’s most popular commercial configurations, but many options might be better suited to different system needs.

Lastly, more research is needed on the ultimate operational benefits and costs of coupled systems. Our system value metrics are based on an optimistic case assuming perfect foresight and a pessimistic case from an implementable day-ahead scheduling algorithm. More sophisticated

methods that incorporate prediction algorithms will be needed to clarify any operational synergies between co-located VRE and battery storage systems compared with independently sited configurations.

7. Acknowledgements

This work was supported by the U.S. Department of Energy (DOE) under Lawrence Berkeley National Laboratory Contract No. DE- AC02-05CH11231. This research used the Lawrence Berkeley National Laboratory computational cluster resource provided by the IT Division at the Lawrence Berkeley National Laboratory (Supported by the Director, Office of Science, Office of Basic Energy Sciences, of the U.S. Department of Energy under Contract No. DE-AC02-05CH11231). We especially thank our DOE sponsors for supporting this research, and in particular Paul Spitsen. We also appreciate early feedback by a number of external advisors on this work. In particular, Caitlin Murphy, Anna Schleifer, Patrick Brown, Mark Ahlstrom, Evan Bierman, and Eric Ela provided very valuable comments. Jarett Zuboy provided substantial editing assistance, and Joe Rand contributed data on coupling within the interconnection queues that appears in the introduction of this paper.

8. Author Contributions

Will Gorman: conceptualization, methodology, software, data curation, formal analysis, visualization, writing - original draft, writing - review & editing. **Cristina Crespo:** methodology, software, formal analysis, visualization, writing - review & editing. **Andrew Mills:** supervision, funding acquisition, conceptualization, methodology, software, writing - review & editing. **James Kim:** data curation, writing - review & editing. **Dev Millstein:** data curation, writing - review & editing. **Ryan Wisner:** conceptualization, writing - review & editing.

9. Competing Interests

The authors declare no competing interests.

10. References

- [1] IEA. Renewables 2020 - Analysis and forecast to 2025 2020:172.
- [2] Larson E, Greig C, Jenkins J, Mayfield E, Pascale A, Zhang C, et al. Net-zero America: Potential Pathways, Infrastructure, and Impacts 2020.
- [3] Mai T, Mulcahy D, Hand MM, Baldwin SF. Envisioning a renewable electricity future for the United States. *Energy* 2014;65:374–86. <https://doi.org/10.1016/j.energy.2013.11.029>.
- [4] Engeland K, Borga M, Creutin J-D, François B, Ramos M-H, Vidal J-P. Space-time variability of climate variables and intermittent renewable electricity production – A review. *Renew Sustain Energy Rev* 2017;79:600–17. <https://doi.org/10.1016/j.rser.2017.05.046>.
- [5] Shaner MR, Davis SJ, Lewis NS, Caldeira K. Geophysical constraints on the reliability of solar and wind power in the United States. *Energy Environ Sci* 2018;11:914–25. <https://doi.org/10.1039/C7EE03029K>.

- [6] Mills A, Wiser R. Changes in the Economic Value of Photovoltaic Generation at High Penetration Levels: A Pilot Case Study of California. *IEEE J Photovolt* 2013;3:1394–402. <https://doi.org/10.1109/JPHOTOV.2013.2263984>.
- [7] Mills A, Wiser R. Changes in the Economic Value of Wind Energy and Flexible Resources at Increasing Penetration Levels in the Rocky Mountain Power Area. *Wind Energy* 2014;17:1711–26. <https://doi.org/10.1002/we.1663>.
- [8] Hirth L. The market value of variable renewables: The effect of solar wind power variability on their relative price. *Energy Econ* 2013;38:218–36. <https://doi.org/10.1016/j.eneco.2013.02.004>.
- [9] Hirth L. Integration costs revisited - An economic framework for wind and solar variability. *Renew Energy* 2015:15.
- [10] Mills A, Seel J, Millstein D, Kim JH, Bolinger M, Gorman W, et al. *Solar-to-Grid: Trends in System Impacts, Reliability, and Market Value in the United States with Data Through 2019*. Berkeley, CA: Lawrence Berkeley National Laboratory (LBNL); 2021.
- [11] Denholm P, Nunemaker J, Gagnon P, Cole W. The Potential for Battery Energy Storage to Provide Peaking Capacity in the United States. *Renew Energy* 2019:45.
- [12] Braff WA, Mueller JM, Trancik JE. Value of storage technologies for wind and solar energy. *Nat Clim Change* 2016;6:964–9. <https://doi.org/10.1038/nclimate3045>.
- [13] Kittner N, Lill F, Kammen DM. Energy storage deployment and innovation for the clean energy transition. *Nat Energy* 2017;2:17125. <https://doi.org/10.1038/nenergy.2017.125>.
- [14] Denholm P, Mai T. Timescales of energy storage needed for reducing renewable energy curtailment. *Renew Energy* 2019;130:388–99. <https://doi.org/10.1016/j.renene.2018.06.079>.
- [15] Ziegler MS, Mueller JM, Pereira GD, Song J, Ferrara M, Chiang Y-M, et al. Storage Requirements and Costs of Shaping Renewable Energy Toward Grid Decarbonization. *Joule* 2019;3:2134–53. <https://doi.org/10.1016/j.joule.2019.06.012>.
- [16] Denholm P, Hand M. Grid flexibility and storage required to achieve very high penetration of variable renewable electricity. *Energy Policy* 2011;39:1817–30. <https://doi.org/10.1016/j.enpol.2011.01.019>.
- [17] Schweppe FC, Caramanis MC, Tabors RD, Bohn RE. *Spot Pricing of Electricity*. Boston, MA: Springer US; 1988. <https://doi.org/10.1007/978-1-4613-1683-1>.
- [18] Bloom A, Novacheck J, Brinkman G, McCalley J, Figueroa-Acevedo A, Jahanbani-Ardakani A, et al. The Value of Increased HVDC Capacity Between Eastern and Western U.S. Grids: The Interconnections Seam Study: Preprint. 2020. <https://doi.org/10.2172/1696787>.
- [19] Brattle, E3, BEAR, Aspen. Senate Bill 350 Study: The Impacts of a Regional ISO-Operated Power Market on California. Prepared for California ISO; 2016.
- [20] Hobbs BF, Oren SS. Three Waves of U.S. Reforms: Following the Path of Wholesale Electricity Market Restructuring. *IEEE Power Energy Mag* 2019;17:73–81. <https://doi.org/10.1109/MPE.2018.2873952>.
- [21] Wiser RH, Bolinger M, Gorman W, Rand J, Jeong S, Seel J, et al. *Hybrid Power Plants: Status of Installed and Proposed Projects*. Berkeley, CA: Lawrence Berkeley National Laboratory; 2020.
- [22] Vejdani S, Grijalva S. The expected revenue of energy storage from energy arbitrage service based on the statistics of realistic market data. 2018 IEEE Tex. Power Energy Conf. TPEC, College Station, TX: IEEE; 2018, p. 1–6. <https://doi.org/10.1109/TPEC.2018.8312055>.

- [23] Mendelsohn M, Weis A. The next big thing: grid-tied batteries. How to maximize value. *Pv Mag USA* 2019. <https://pv-magazine-usa.com/2019/03/04/the-next-big-thing-grid-tied-batteries-how-to-maximize-value/> (accessed March 25, 2021).
- [24] Gorman W, Mills A, Bolinger M, Wiser R, Singhal NG, Ela E, et al. Motivations and options for deploying hybrid generator-plus-battery projects within the bulk power system. *Electr J* 2020;33:106739. <https://doi.org/10.1016/j.tej.2020.106739>.
- [25] Ericson S, Anderson K, Engel-Cox J, Jayaswal H, Arent D. Power couples: The synergy value of battery-generator hybrids. *Electr J* 2018;31:51–6. <https://doi.org/10.1016/j.tej.2017.12.003>.
- [26] Murphy CA, Schleifer A, Eurek K. A taxonomy of systems that combine utility-scale renewable energy and energy storage technologies. *Renew Sustain Energy Rev* 2021;139:110711. <https://doi.org/10.1016/j.rser.2021.110711>.
- [27] Ela EG, Singhal NG. *Energy Storage Integration into Electricity Markets: Current Status and Ongoing Research* 2019.
- [28] Joskow PL. Comparing the Costs of Intermittent and Dispatchable Electricity Generating Technologies. *Am Econ Rev* 2011;101:238–41. <https://doi.org/10.1257/aer.101.3.238>.
- [29] Joskow PL. Capacity payments in imperfect electricity markets: Need and design. *Util Policy* 2008;16:159–70. <https://doi.org/10.1016/j.jup.2007.10.003>.
- [30] Borenstein S. *The Market Value and Cost of Solar Photovoltaic Electricity Production*. Berkeley, CA: UC Energy Institute; 2008.
- [31] Millstein D, Wiser R, Mills A, Bolinger M, Seel J, Jeong S. *Solar and Wind Grid-System Value in the United States: The Impact of Transmission Congestion, Generation Profiles, and Curtailment* n.d.
- [32] Bradbury K, Pratson L, Patiño-Echeverri D. Economic viability of energy storage systems based on price arbitrage potential in real-time U.S. electricity markets. *Appl Energy* 2014;114:512–9. <https://doi.org/10.1016/j.apenergy.2013.10.010>.
- [33] McConnell D, Forcey T, Sandiford M. Estimating the value of electricity storage in an energy-only wholesale market. *Appl Energy* 2015;159:422–32. <https://doi.org/10.1016/j.apenergy.2015.09.006>.
- [34] Kim JH, Mills AD, Wiser R, Bolinger M, Gorman W, Montanes CC, et al. -Enhancing the Value of Solar Energy as Solar and Storage Penetrations Increase. *SSRN Electron J* 2020. <https://doi.org/10.2139/ssrn.3732356>.
- [35] Byrne RH, Nguyen TA, Copp DA, Concepcion RJ, Chalamala BR, Gyuk I. Opportunities for Energy Storage in CAISO: Day-Ahead and Real-Time Market Arbitrage. 2018 Int. Symp. Power Electron. Electr. Drives Autom. Motion SPEEDAM, 2018, p. 63–8. <https://doi.org/10.1109/SPEEDAM.2018.8445408>.
- [36] McPherson M, McBennett B, Sigler D, Denholm P. Impacts of storage dispatch on revenue in electricity markets. *J Energy Storage* 2020;31:101573. <https://doi.org/10.1016/j.est.2020.101573>.
- [37] DiOrio N, Denholm P, Hobbs WB. A model for evaluating the configuration and dispatch of PV plus battery power plants. *Appl Energy* 2020;262:114465. <https://doi.org/10.1016/j.apenergy.2019.114465>.
- [38] Byrne RH, Nguyen TA, Headley A, Wilches-Betnal F, Concepcion R, Trevizan RD. Opportunities and Trends for Energy Storage Plus Solar in CAISO: 2014-2018. 2020 IEEE Power Energy Soc. Gen. Meet. PESGM, Montreal, QC: IEEE; 2020, p. 1–5. <https://doi.org/10.1109/PESGM41954.2020.9281883>.

- [39] Mills AD, Rodriguez P. A simple and fast algorithm for estimating the capacity credit of solar and storage. *Energy* 2020;210:118587. <https://doi.org/10.1016/j.energy.2020.118587>.
- [40] Schleifer AH, Murphy CA, Cole WJ, Denholm PL. The evolving energy and capacity values of utility-scale PV-plus-battery hybrid system architectures. *Adv Appl Energy* 2021;2:100015. <https://doi.org/10.1016/j.adapen.2021.100015>.
- [41] Denholm P, Eichman J, Margolis R. Evaluating the Technical and Economic Performance of PV Plus Storage Power Plants. Golden, CO: National Renewable Energy Laboratory (NREL); 2017.
- [42] Cole W, Gates N, Mai T, Greer D, Das P. 2019 Standard Scenarios Report: A U.S. Electric Sector Outlook n.d.:36.
- [43] Sepulveda NA, Jenkins JD, de Sisternes FJ, Lester RK. The Role of Firm Low-Carbon Electricity Resources in Deep Decarbonization of Power Generation. *Joule* 2018;2:2403–20. <https://doi.org/10.1016/j.joule.2018.08.006>.
- [44] MacDonald AE, Clack CTM, Alexander A, Dunbar A, Wilczak J, Xie Y. Future cost-competitive electricity systems and their impact on US CO2 emissions. *Nat Clim Change* 2016;6:526–31. <https://doi.org/10.1038/nclimate2921>.
- [45] McCalley J, Caspary J, Clack C, Galli W, Marquis M, Osborn D, et al. Wide-Area Planning of Electric Infrastructure: Assessing Investment Options for Low-Carbon Futures. *IEEE Power Energy Mag* 2017;15:83–93. <https://doi.org/10.1109/MPE.2017.2729178>.
- [46] Clack CTM, Qvist SA, Apt J, Bazilian M, Brandt AR, Caldeira K, et al. Evaluation of a proposal for reliable low-cost grid power with 100% wind, water, and solar. *Proc Natl Acad Sci* 2017;114:6722–7. <https://doi.org/10.1073/pnas.1610381114>.
- [47] Jenkins JD, Luke M, Thernstrom S. Getting to Zero Carbon Emissions in the Electric Power Sector. *Joule* 2018;2:2498–510. <https://doi.org/10.1016/j.joule.2018.11.013>.
- [48] Bistline J, Cole W, Damato G, DeCarolis J, Frazier W, Linga V, et al. Energy storage in long-term system models: a review of considerations, best practices, and research needs. *Prog Energy* 2020;2:032001. <https://doi.org/10.1088/2516-1083/ab9894>.
- [49] MISO. MISO’s Renewable Integration Impact Assessment (RIIA) Summary Report. 2021.
- [50] Maloney P, Chitkara P, McCalley J, Hobbs BF, Clack CTM, Ortega-Vazquez MA, et al. Research to develop the next generation of electric power capacity expansion tools: What would address the needs of planners? *Int J Electr Power Energy Syst* 2020;121:106089. <https://doi.org/10.1016/j.ijepes.2020.106089>.
- [51] Eicke A, Khanna T, Hirth L. Locational Investment Signals: How to Steer the Siting of New Generation Capacity in Power Systems? *Energy J* 2020;41. <https://doi.org/10.5547/01956574.41.6.aeic>.
- [52] Borowski PF. Zonal and Nodal Models of Energy Market in European Union. *Energies* 2020;13:4182. <https://doi.org/10.3390/en13164182>.
- [53] Wisner R, Bolinger M, Hoen B, Millstein D, Rand J, Barbose G, et al. Wind Energy Technology Data Update: 2020 Edition. Berkeley, CA: Lawrence Berkeley National Laboratory; 2020.
- [54] Wisner RH, Mills AD, Seel J, Levin T, Botterud A. Impacts of Variable Renewable Energy on Bulk Power System Assets, Pricing, and Costs. Berkeley, CA: Lawrence Berkeley National Laboratory; 2017.
- [55] EIA. Annual Electric Power Industry Report, Form EIA-861 detailed data files 2019. <https://www.eia.gov/electricity/data/eia861/> (accessed April 2, 2021).

- [56] EIA. Electric Power Monthly with data for December 2019. 2020.
- [57] Energy Storage Association. Status of Hybrid Resource Initiatives in U.S. Organized Wholesale Markets 2020.
- [58] Stephen G, Hale E, Cowiestoll B. Managing Solar Photovoltaic Integration in the Western United States: Resource Adequacy Considerations. 2020. <https://doi.org/10.2172/1755686>.
- [59] CPUC. Resource Adequacy Webpage n.d. <https://www.cpuc.ca.gov/ra/> (accessed March 26, 2021).
- [60] FERC. FERC EQR data viewer n.d. <https://eqrreportviewer.ferc.gov/> (accessed March 26, 2021).
- [61] He G, Chen Q, Moutis P, Kar S, Whitacre JF. An intertemporal decision framework for electrochemical energy storage management. *Nat Energy* 2018;3:404–12. <https://doi.org/10.1038/s41560-018-0129-9>.
- [62] Forrest J, Hall J. COIN-OR: Computational Infrastructure for Operations Research. COIN-Comput Infrastruct Oper Res n.d. <https://www.coin-or.org/> (accessed January 5, 2021).
- [63] Dunning I, Huchette J, Lubin M. JuMP: A Modeling Language for Mathematical Optimization. *SIAM Rev* 2017;59:295–320. <https://doi.org/10.1137/15M1020575>.
- [64] EIA. Form EIA-860 detailed data with previous form data (EIA-860A/860B) n.d. <https://www.eia.gov/electricity/data/eia860/> (accessed January 5, 2021).
- [65] Sengupta M, Xie Y, Lopez A, Habte A, Maclaurin G, Shelby J. The National Solar Radiation Data Base (NSRDB). *Renew Sustain Energy Rev* 2018;89:51–60. <https://doi.org/10.1016/j.rser.2018.03.003>.
- [66] National Renewable Energy Laboratory. Home - System Advisor Model (SAM) n.d. <https://sam.nrel.gov/> (accessed January 5, 2021).
- [67] Wiser R, Millstein D, Bolinger M, Jeong S, Mills A. The hidden value of large-rotor, tall-tower wind turbines in the United States. *Wind Eng* 2020:0309524X20933949.
- [68] Copernicus Climate Change Service. ERA5: Fifth generation of ECMWF atmospheric reanalyses of the global climate. ECMWF 2017. <https://www.ecmwf.int/en/forecasts/dataset/ecmwf-reanalysis-v5> (accessed January 30, 2021).
- [69] ABB. Velocity Suite n.d. <https://www.hitachiabb-powergrids.com/offering/product-and-system/enterprise/energy-portfolio-management/market-intelligence-services/abb-velocity-suite> (accessed January 5, 2021).
- [70] Bolinger M, Seel J, Robson D, Warner C. Utility-Scale Solar Data Update: 2020 Edition. Berkeley, CA: Lawrence Berkeley National Laboratory (LBNL); 2020.
- [71] Denholm PL, Sun Y, Mai TT. An Introduction to Grid Services: Concepts, Technical Requirements, and Provision from Wind. 2019. <https://doi.org/10.2172/1493402>.
- [72] Larsen C. Solar Plus energy storage: A guide to maximizing production and profit with a DC converter. Dynapower Company; 2019.
- [73] Potomac Economics. 2019 State of the Market Report For the ERCOT Electricity Markets. Potomac Economics, Ltd; 2020.
- [74] Cole WJ, Frazier A. Cost Projections for Utility-Scale Battery Storage. 2019. <https://doi.org/10.2172/1529218>.
- [75] Fu R, Remo T, Margolis R. 2018 U.S. Utility-Scale Photovoltaics-Plus-Energy Storage System Costs Benchmark. National Renewable Energy Laboratory; 2018.
- [76] Lopez A, Roberts B, Heimiller D, Blair N, Porro G. U.S. Renewable Energy Technical Potentials: A GIS-Based Analysis. *Renew Energy* 2012:40.

- [77] Tegen S, Lantz E, Mai T, Heimiller D, Hand M, Ibanez E. An Initial Evaluation of Siting Considerations on Current and Future Wind Deployment. 2016. <https://doi.org/10.2172/1279497>.
- [78] Seel J, Mills A, Wiser R. Impacts of High Variable Renewable Energy Futures on Wholesale Electricity Prices, and on Electric-Sector Decision Making. Berkeley, CA: Lawrence Berkeley National Laboratory; 2018.
- [79] Clifton A, Smith A, Fields M. Wind Plant Preconstruction Energy Estimates. Current Practice and Opportunities. 2016. <https://doi.org/10.2172/1248798>.

11. Supplementary Information

11.1. ADDITIONAL MODEL DETAILS

More details on the day-ahead schedule algorithm

The day-ahead schedule algorithm differs from the perfect foresight algorithm in three ways: 1) the renewable resource and energy pricing inputs of the optimization program, 2) the operation of renewable generation curtailment, and 3) the energy revenue calculation. First, we take as inputs an hourly time series of day-ahead energy market prices (instead of the real-time prices used in the perfect foresight case) and an hourly time series of renewable capacity factors shifted forward 24 hours, such that each hour in the modeling year is assigned the capacity factor corresponding to the day before, hence using the renewable resource of a given day as an estimate for the day after. We use these inputs in the optimization program described in Section 3.2 to generate the coupled project and standalone storage plants' optimal schedules.

We post-process the results to assess the optimal schedules' operational feasibility using the actual renewable capacity factor time series. When real-time prices are negative, the renewable resource is curtailed to zero, regardless of whether there is enough storage capacity to charge the battery further. When the charging and discharging of the battery in the optimal schedule are unfeasible under the actual renewable resource, it is revised to account for the actual renewable generation, resulting in a corrected dispatch. When grid charging is allowed, grid imports and exports will be modified to satisfy the optimal schedule. We calculate the revenue for the coupled project and standalone storage plant by multiplying the real-time energy market prices by the corrected dispatch of the plants.

Debiasing of wind speeds

The first step in the wind debiasing process was to take raw ERA5 wind speeds at model levels ranging up to roughly 140 meters above ground and interpolate these wind speeds to the hub height of each plant. We then estimated wind energy at hub height so as to best match recorded generation. We used a power curve that was selected to match the technology found at each wind

plant (power curves were compiled from thewindpower.net database). Average losses were applied to the output of the power curve, including a 2% loss for availability, and a 15% loss for electrical, wake, and other losses. These losses were based on estimates in Clifton et al. [79]. Additionally, a small (<10%) adjustment was made to account for lower air density associated with elevation. A simplification here is that these losses were specified as constant across hours, though some of the losses would, in actuality, vary by hour.

An iterative process was then used to find the implied long-term average wind speed at each site, and develop a debiasing scaler for ERA5 wind time series at each site. The plant-specific modeled generation was compared to recorded generation from months 13-60 of each plant. Wind speeds were then iteratively scaled and run through the plant-specific power curve until the average generation matched the recorded average generation over the selected period. This process created one scaler per plant in our sample. For newer plants, we allowed the generation matching to occur over fewer months, requiring at least 1 year of data to match on, or at least 2 years then of project life. The first year of each project was not included in this debiasing process to account for teething issues and phased deployment of turbines.

After a scaler was found for each plant, it was applied to all hours and years of wind speed. This scaling allows long-term model bias from ERA5 to be removed. Finally, these debiased wind speeds were combined with a common turbine curve using a 2018 average turbine (2.43 MW, 115.6 m rotor) built from SAM [66]. The power curve fit is based on a third-order polynomial curve with data between the cut-in and cut-out wind speed. This output is the wind power estimates at existing wind plants using a common power curve that we seek.

Expanded optimization model with ancillary service value

Terms bolded in blue below represent the additional terms added to the original optimization formulation to take into account regulation reserve values.

Objective function:

$$Max \sum_1^{8760} [(P_{rt} + P_c/N * NL_m) * (G_i + \gamma R_i)] + [R_i * P_{as}] - [D_p * (B_d + B_c + \gamma R_i)] \quad (\text{Eq. 1})$$

Subject to:

Beginning state of charge: $S_0 = 0$ (Eq. 2)

State of charge range: $0 \leq S_k \leq S_{max}$ (Eq. 3)

Power in rate: $0 \leq B_c(k) \leq B_{max}$ (Eq. 4)

Power out rate: $0 \leq B_d(k) \leq B_{max}$ (Eq. 5)

Non-simultaneity rule: $B_d(k) + B_c(k) \leq B_{max}$ (Eq. 6)

Battery state of charge: $S_{k+1} = S_k + \left[\eta B_c(k) - \frac{B_d(k)}{\eta} \right]$ (Eq. 7)

AC-grid limits: $-I_g B_{max} \leq G_i(k) \leq POI$ (Eq. 8)

AC-grid balance: $G_i(k) = W(k) + B_d(k) - B_c(k)$ (Eq. 9)

Regulation constraint: $R_i + B_c(k) \leq B_{max}$ (Eq. 10)

Regulation constraint: $R_i + B_d(k) \leq B_{max}$ (Eq. 11)

Regulation AC constraint: $R_i + |G_i(k)| \leq POI$ (Eq. 12)

Where,

P_r = hourly real time electricity (\$/MWh)

P_c = capacity price (\$/MW)

NL_m = hourly indicator (0 or 1) for top 100 net-load hour for given market

N = number of top net-load hours, set to 100 in this analysis (h)

G_i = hourly net electricity profile of coupled or storage system (MWh)¹⁶

γ = regulation energy served fraction (%)

R_i = hourly regulation reserve profile of coupled or storage system (MWh)

P_{as} = hourly regulation reserve price (\$/MWh)

D_p = degradation penalty (\$/MWh)

B_d = battery discharging (MWh)

B_c = battery charging (MWh)

B_{max} = battery max power capacity (MW)

S_k = battery state of charge at time step k (MWh)

S_{max} = total energy capacity of battery (MWh)

η = battery one-way efficiency (%)

I_g = binary indicator to allow grid charging (1 allows grid charging, 0 restricts charging to available VRE)

POI = point of interconnection limit

W_k = power generated from renewable resource at time step k

Expanded optimization model for DC-coupled projects

Terms bolded in blue below represent the additional/changed terms added to the original optimization formulation to take into account DC-coupling.

¹⁶ For battery systems, this is more explicitly written as $B_d - B_c$.

Objective function:

$$\text{Max } \sum_1^{8760} [(P_{rt} + P_c/N * NL_m) * G_{ac}] - [D_p * (B_d + B_c)] \quad (\text{Eq. 13})$$

Subject to:

Beginning state of charge: $S_0 = 0$ (Eq. 14)

State of charge range: $0 \leq S_k \leq S_{max}$ (Eq. 15)

Power in rate: $0 \leq B_c(k) \leq \frac{B_{max}}{\alpha}$ (Eq. 16)

Power out rate: $0 \leq B_d(k) \leq \frac{B_{max}}{\alpha}$ (Eq. 17)

Non-simultaneity rule: $B_d(k) + B_c(k) \leq \frac{B_{max}}{\alpha}$ (Eq. 18)

Battery state of charge: $S_{k+1} = S_k + \left[\mu B_c(k) - \frac{B_d(k)}{\mu} \right]$ (Eq. 19)

AC-grid limits: $-I_g B_{max} \leq G_{ac}(k) \leq POI$ (Eq. 20)

Inverter-out: $G_{out-ac}(k) = G_{out-dc}(k) * \alpha$ (Eq. 21)

Inverter-in: $G_{in-ac}(k) = G_{in-dc}(k) * \alpha$ (Eq. 22)

DC-grid balance: $G_{in-dc}(k) = G_{out-dc}(k) + B_c(k) - W(k) - B_d(k)$ (Eq. 23)

AC-grid balance: $G_{ac}(k) = G_{out-ac}(k) - G_{in-ac}(k)$ (Eq. 24)

Where,

P_{rt} = hourly real time electricity (\$/MWh)

P_c = capacity price (\$/MW)

NL_m = hourly indicator (0 or 1) for top 100 net-load hour for given market

N = number of top net-load hours, set to 100 in this analysis (h)

G_{ac} = hourly AC net electricity profile of DC-coupled system (MWh)

D_p = degradation penalty (\$/MWh)

B_d = battery discharging (MWh)

B_c = battery charging (MWh)

B_{max} = battery max power capacity (MW)

α = inverter efficiency (%)

S_k = battery state of charge at time step k (MWh)

S_{max} = total energy capacity of battery (MWh)

μ = battery efficiency without inverter losses (%)

I_g = binary indicator to allow grid charging (1 allows grid charging, 0 restricts charging to available VRE)
 POI = point of interconnection limit
 G_{out-ac} = energy out from the AC inverter (MWh)
 G_{out-dc} = energy out from the battery and/or PV system (MWh)
 G_{in-ac} = energy in from the AC inverter, that is the grid (MWh)
 G_{in-dc} = energy into the battery from the AC inverter and/or PV system (MWh)
 W_k = DC power generated from solar resource at time step k

11.2. STORAGE VALUE ADDER SENSITIVITIES

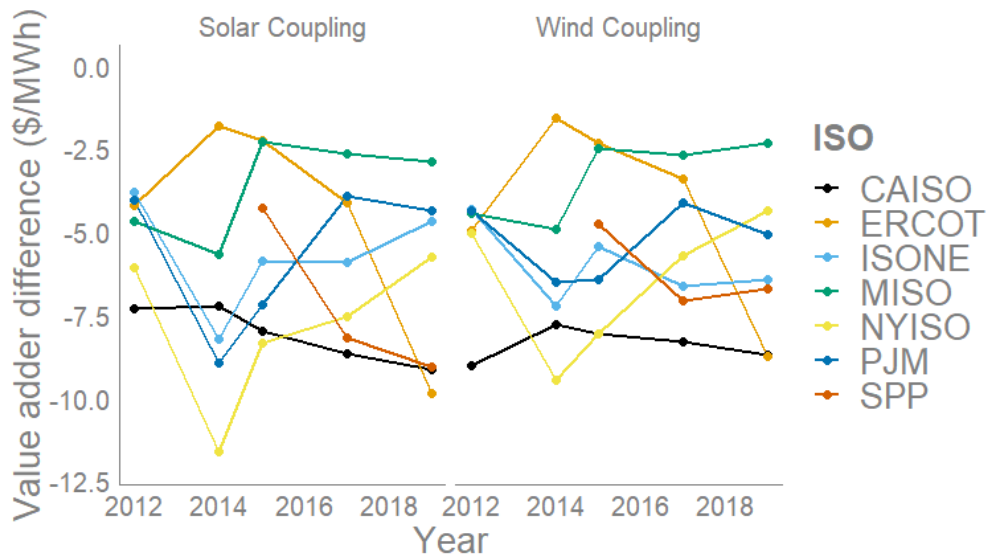


Figure A-11-1: Storage value adder difference using day-ahead schedule algorithm

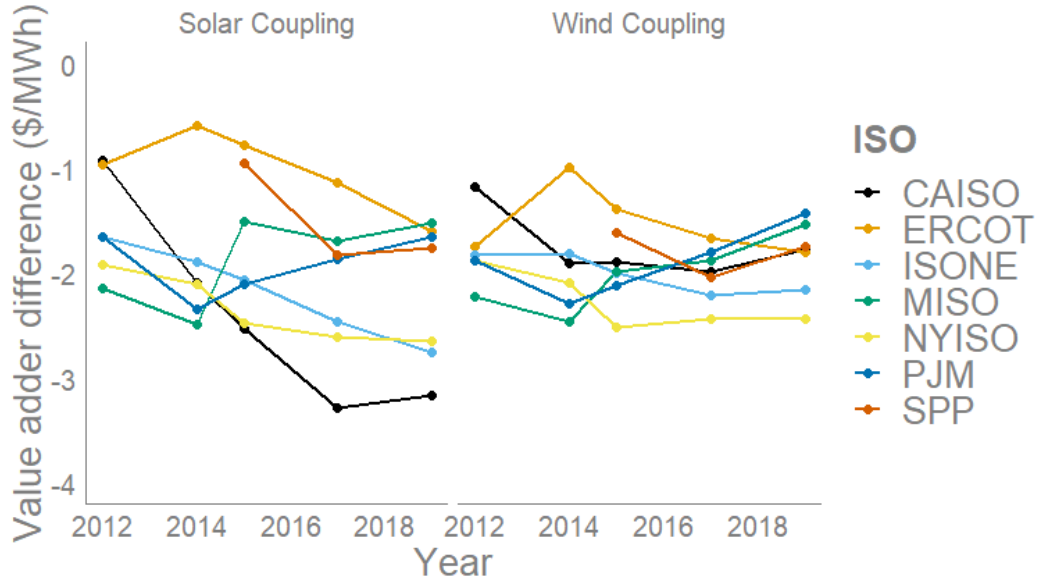


Figure A-11-2: Storage value adder difference using \$25/MWh degradation penalty

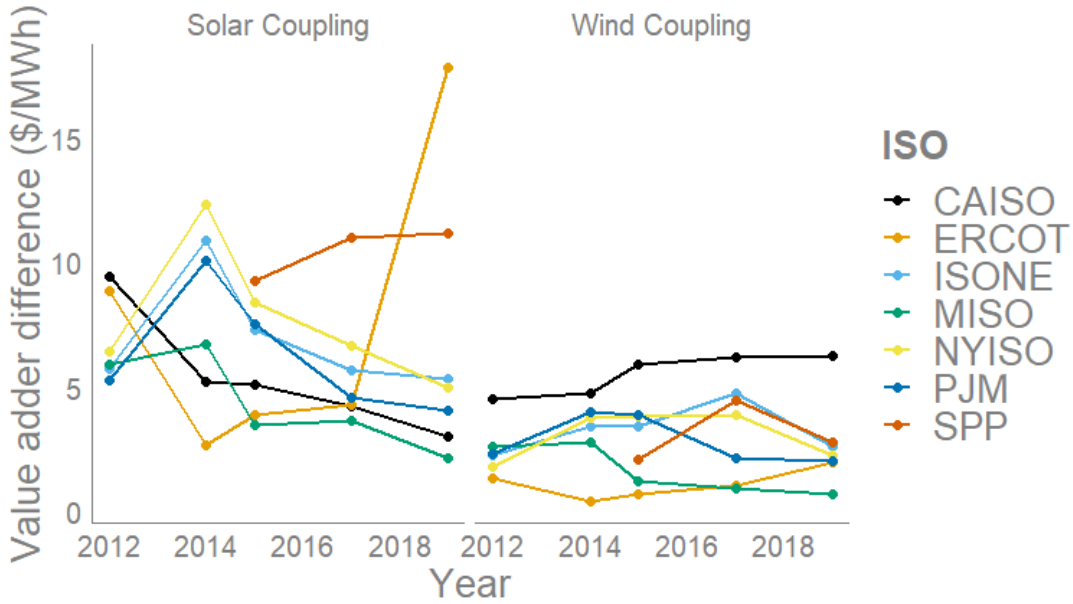


Figure A-11-3: Storage value adder difference while allowing grid charging and increasing POI limit

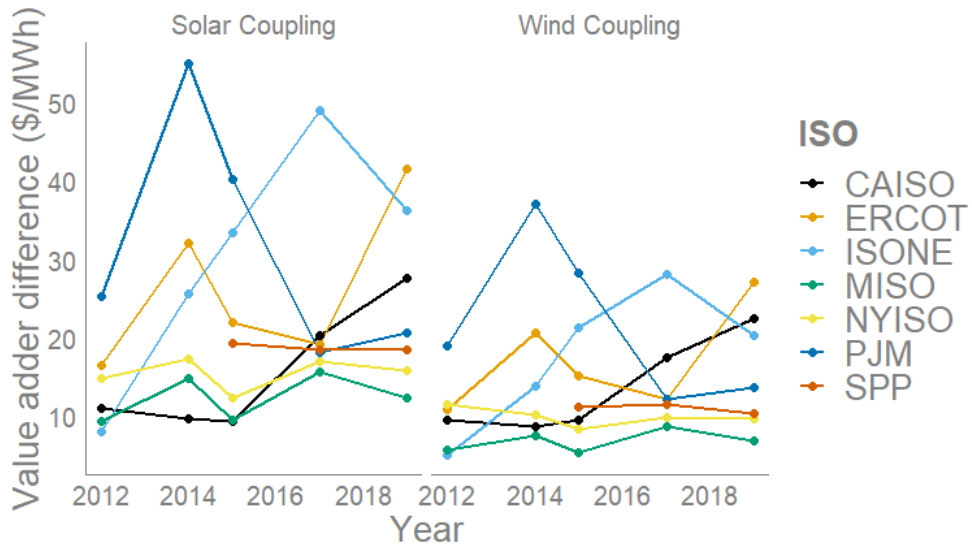


Figure A-11-4: Storage value adder difference with regulation value included

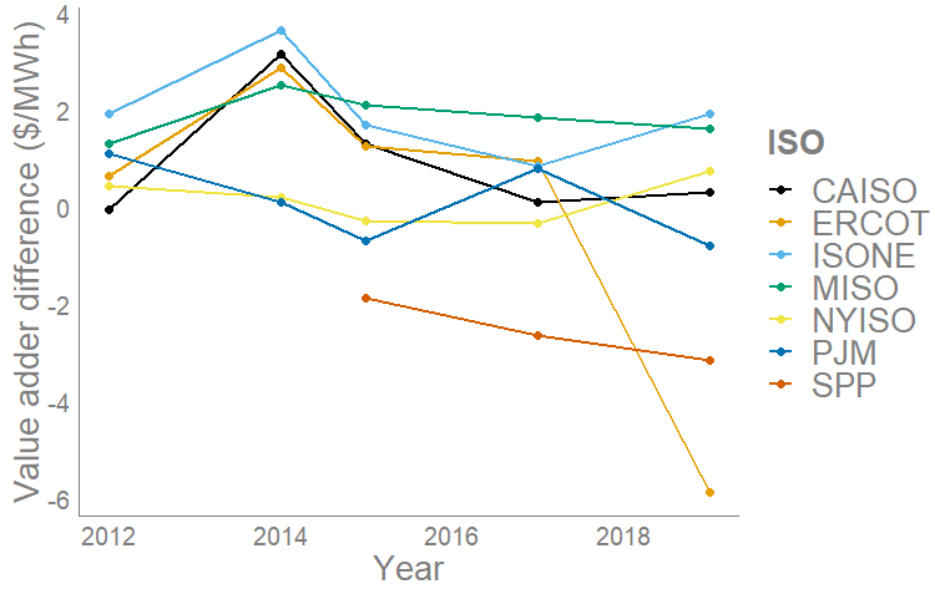


Figure A-11-5: Storage value adder difference with 1.7-DC coupled

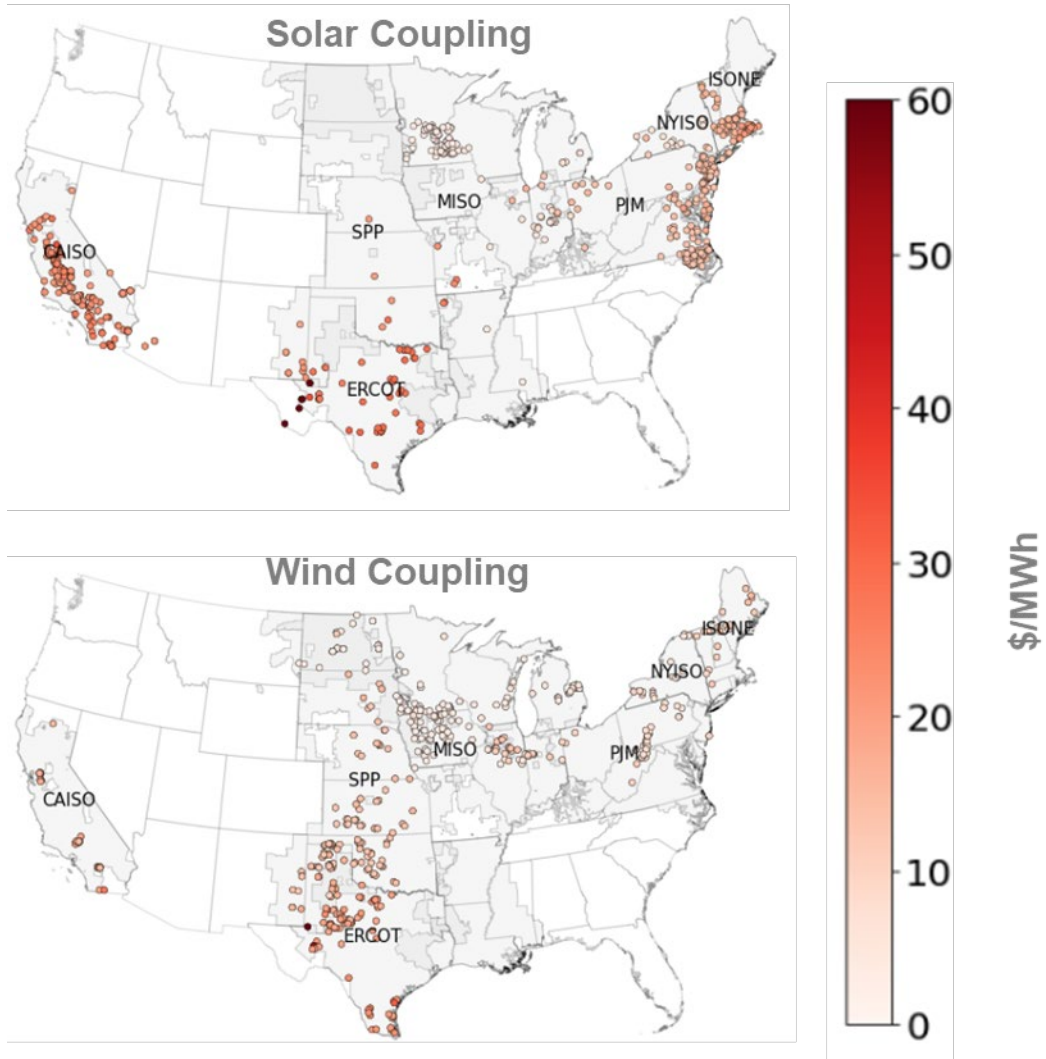


Figure A-11-6: Absolute storage value adder for all wind and solar nodes in 2019

11.3. COUPLING PENALTY SENSITIVITIES

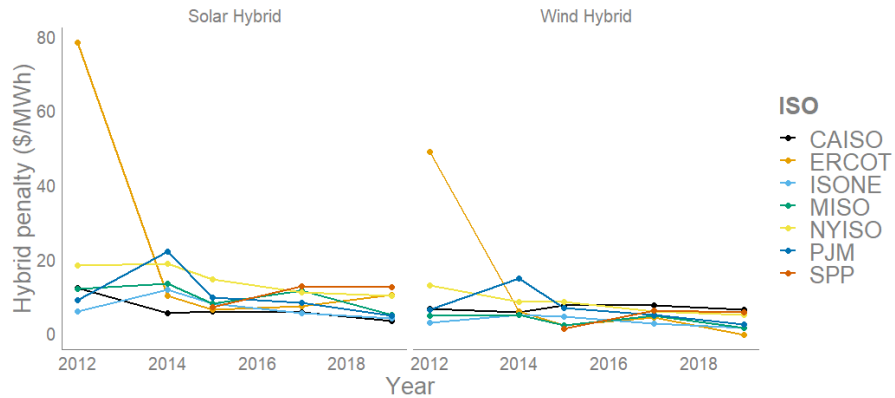


Figure A-11-7: Coupling penalty with low end high volatile node

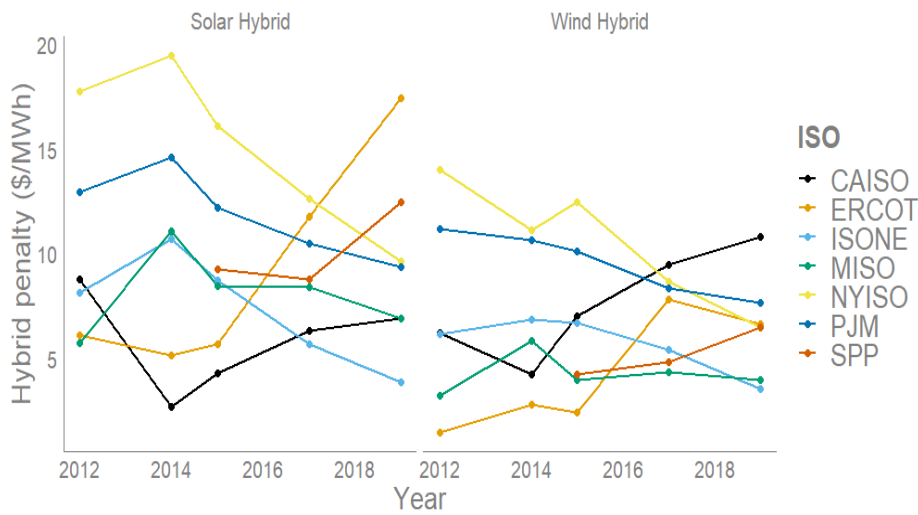


Figure A-11-8: Coupling penalty assuming day-ahead schedule algorithm

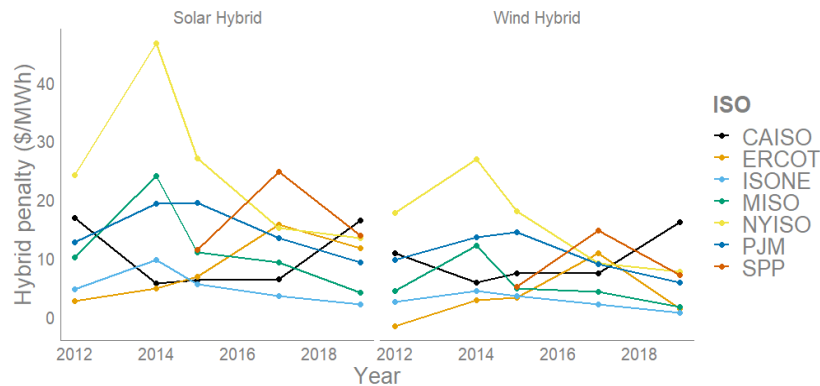


Figure A-11-9: Coupling penalty with \$25/MWh degradation penalty

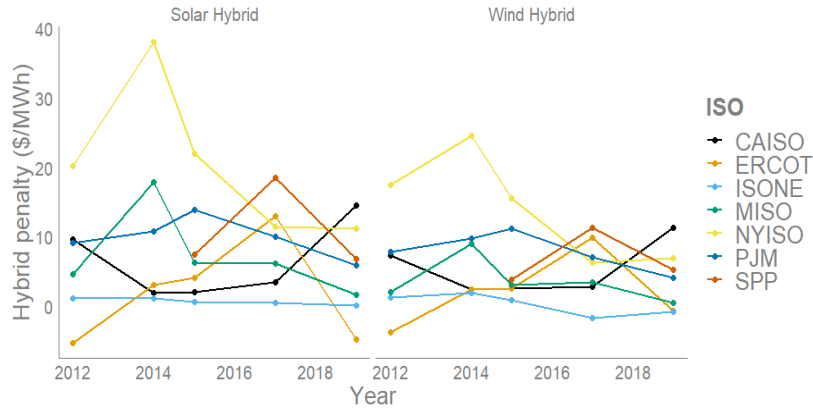


Figure A-11-10: Coupling penalty while allowing grid charging and increasing the POI limit

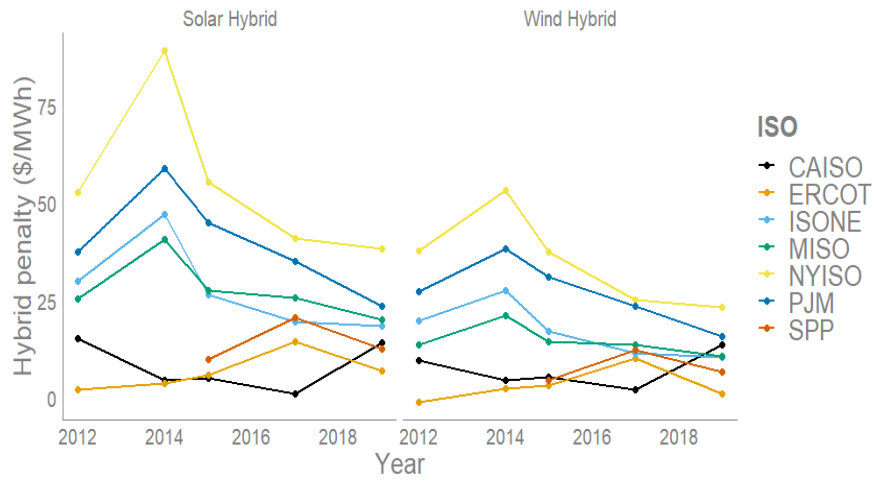


Figure A-11-11: Coupling penalty with regulation value included

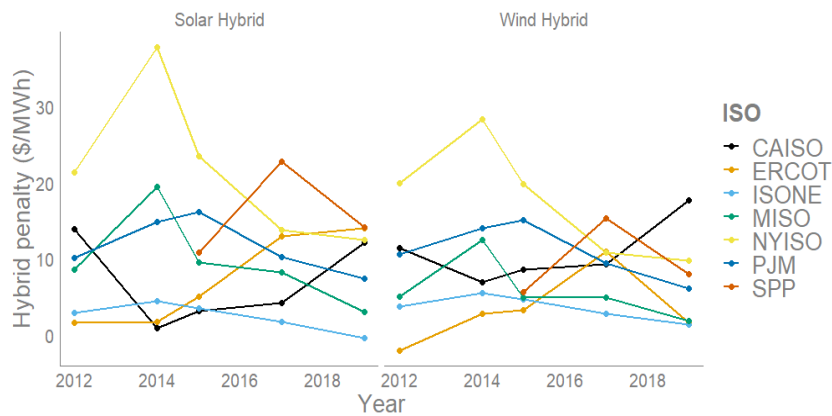


Figure A-11-12: Coupling penalty with 1.7 DC-coupled system

11.4. NODAL METRICS

The figure below plots the correlation between a node’s annual standard deviation, the metric we use to select high-value nodes, and the corresponding standalone storage value from our optimization calculation. These figures show high correlations between these two variables across all node types, confirming the appropriateness of our high-value node identification strategy. The nodes we did not consider showed similar standard deviation distributions to the wind and solar nodes (following figure).

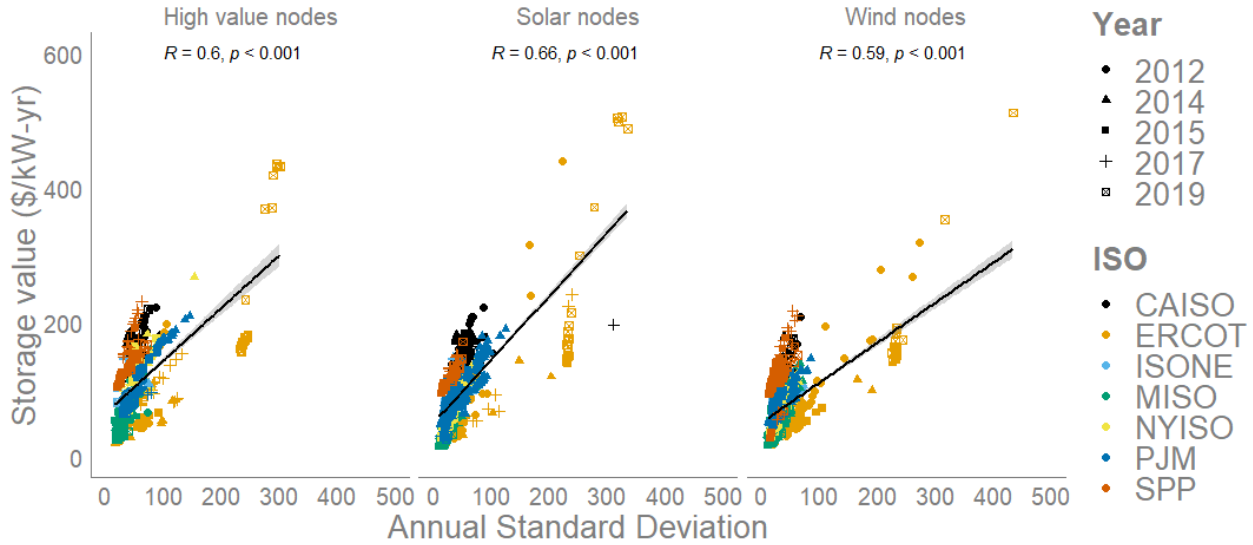


Figure A-11-13: Comparison of storage revenue to pricing standard deviation

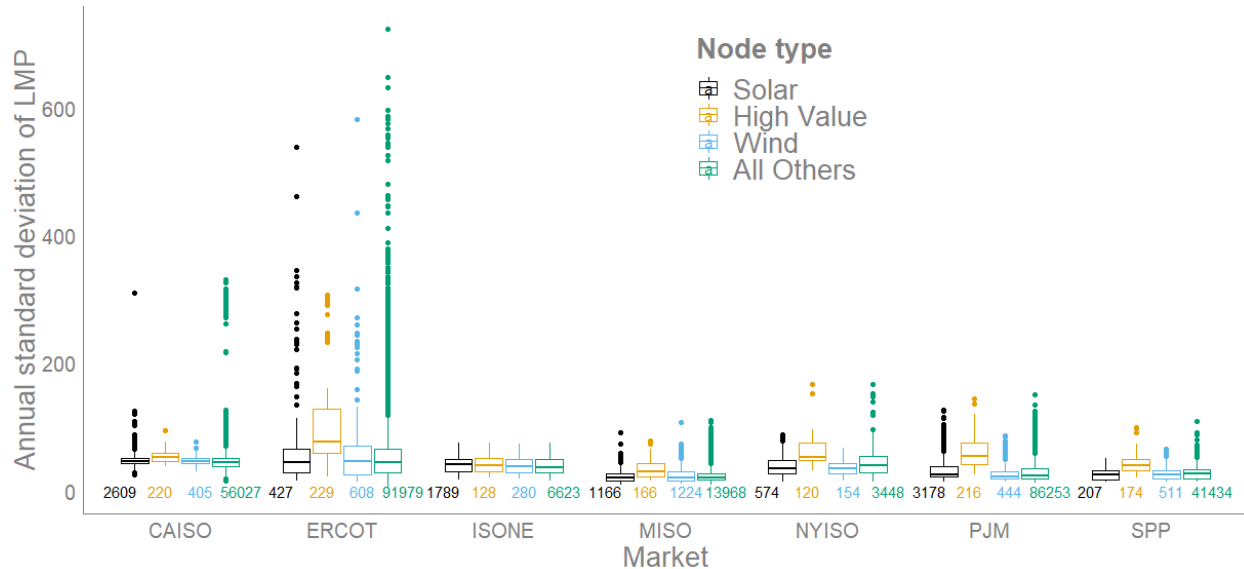


Figure A-11-14: Standard deviation of all nodes in 7 U.S. electricity markets from 2012-2019, with total unique node-year count



Figure A-11-15: Locations of highest-volatility nodes selected in sample



Figure A-11-16: Locations of 30th most volatile node selected in sample